

12-2017

An analysis of oxidative damage to lactate dehydrogenase in context of neurodegeneration and catechol-based phenolic antioxidant chemistry

Lydia Boike

Follow this and additional works at: <https://scholarworks.wm.edu/honorstheses>



Part of the [Biochemistry Commons](#)

Recommended Citation

Boike, Lydia, "An analysis of oxidative damage to lactate dehydrogenase in context of neurodegeneration and catechol-based phenolic antioxidant chemistry" (2017). *Undergraduate Honors Theses*. Paper 1144. <https://scholarworks.wm.edu/honorstheses/1144>

This Honors Thesis is brought to you for free and open access by the Theses, Dissertations, & Master Projects at W&M ScholarWorks. It has been accepted for inclusion in Undergraduate Honors Theses by an authorized administrator of W&M ScholarWorks. For more information, please contact scholarworks@wm.edu.

An analysis of oxidative damage to lactate dehydrogenase in context of neurodegeneration and catechol-based phenolic antioxidant chemistry

A thesis submitted in partial fulfillment of the requirement
for the degree of Bachelor of Science in Chemistry from
the College of William & Mary

By

Lydia Eulalie Boike

Accepted for _____

Dr. Lisa Landino, Director

Dr. Christopher Abelt

Dr. Daniel Cristol

Dr. Douglas Young

December 6, 2017

TABLE OF CONTENTS

ABSTRACT	3
INTRODUCTION	4
BACKGROUND	7
Alzheimer's disease pathology.....	7
Antioxidants: scavengers of ROS.....	12
Energy production in disease states.....	16
Protein thiol chemistry.....	19
MATERIALS and METHODOLOGY	23
Materials.....	23
Protein Purification.....	24
Preparation of chicken muscle, chicken liver, and beef liver extracts.....	25
Preparation of tea and hops extracts.....	25
Oxidation of LDH and ADH samples.....	25
Modifications of oxidation process.....	26
LDH kinetics procedure.....	26
ADH kinetics procedure.....	27
IAF labeling procedure and SDS-PAGE.....	28
RESULTS and DISCUSSION	30
Rabbit muscle LDH kinetics.....	30
Rabbit muscle LDH and HOCl.....	31
Protection of LDH from HOCl damage.....	35
Reduction of oxidized LDH with TCEP.....	37
Oxidation of LDH with HOCl in chicken and beef liver extracts.....	38
Oxidation of LDH and ADH with ortho-quinones.....	39
Glutathione competition with oxidants.....	45
CONCLUSION	46
APPENDIX	48
Table of frequently used compounds, their structures, and abbreviations.....	48
Yeast ADH structure with labeled important amino acids.....	50
All phenolic compounds oxidized and tested for inhibition of LDH and ADH.....	52
Rabbit muscle LDH amino acid sequence.....	57
Yeast ADH amino acid sequence.....	58
REFERENCES	59

ABSTRACT

Lactate dehydrogenase, a redox-active enzyme with five reactive cysteine residues, reversibly converts pyruvate to lactate during anaerobic glycolysis. In the case of certain disease states, when oxygen levels are low or increased oxidative stress damages mitochondrial respiration, cells must rely heavily on anaerobic glycolysis for ATP production. This is true of Alzheimer's disease, Parkinson's disease, ALS, and many cancers. Diseased cells upregulate anaerobic glycolytic enzymes - particularly LDH – to produce enough energy to survive. Upregulated LDH plays a key role because as it produces lactate, it also replenishes NAD^+ , allowing for high levels of glycolysis to continue uninterrupted. Despite research into the function of LDH as a glycolytic enzyme, little focus has been allocated to its role outside of glycolysis and its interaction with reactive oxygen species and other cysteine reactive compounds – knowledge of which could illuminate further disease mechanics.

For this project, we first investigated the effects of bleach (HOCl) – a common reactive oxygen species found elevated in Alzheimer's disease – on LDH structure and function. We then examined the effects of oxidized plant-derived phenolic antioxidants on LDH activity. Research shows that catechol-based antioxidants are readily oxidized by radicals to quinones. These quinones can further react with protein thiols, demonstrating the potential for beneficial antioxidants to become damaging pro-oxidants, and thus prompting our investigation into their reactivity with LDH cysteine residues. We compared our results with LDH to those obtained using alcohol dehydrogenase (ADH), a model protein that also contains readily oxidized cysteine residues. In our work we utilized UV/Vis spectroscopy, fluorescence spectroscopy, and SDS-PAGE techniques to examine how LDH and ADH structure and function changed when respective available protein thiols were reacted with HOCl or oxidized plant-derived phenolic antioxidants. Resulting data confirms these compounds inhibit LDH and ADH activity, strongly suggesting that modification of key cysteine residues occurs, changing the conformation of the protein.

INTRODUCTION

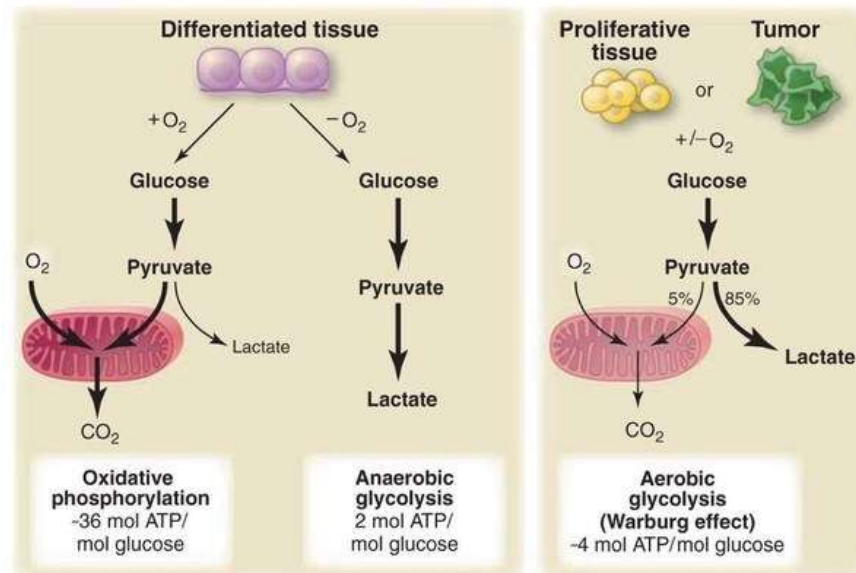
Glycolytic enzymes including lactate dehydrogenase (LDH), glyceraldehyde-3-phosphate dehydrogenase (GAPDH), and pyruvate kinase (PK) are abundant in nearly all cell types and all contain reduced cysteine residues which are readily oxidized by various compounds found both endogenously in cells and exogenously in medicines, pollutants, and cancerous agents (Foley et. al. 2014). Little research has characterized the dynamic and diverse functions of these enzymes in disease contexts. In this paper, we investigated LDH in the context of Alzheimer's disease (AD) and ageing. We examined LDH with respect to the following reaction types: 1. HOCl modification of cysteine residues, 2. glutathione scavenging of radicals and modification of cysteine residues, and 3. the potential for antioxidants to become pro-oxidants and bind irreversibly to cysteine residues. In the third case, we specifically investigated the oxidative capabilities of ortho-quinones, or oxidized catechol-based derivatives (common antioxidants found in all or most plants). We then compared our results with similar experiments done in our lab on alcohol dehydrogenase (ADH), a model protein found in yeast cells.

Cellular disease states depend on tightly regulated energy production. Thus, enzymes involved in energy production – such as glycolytic enzymes – are very important in maintaining disease conditions. For example, in tumor cells where oxygen is not readily available, the cell cannot rely on mitochondrial respiration (in which oxygen is required). Glycolysis levels are elevated to compensate for expected energy loss. This is called the Warburg effect (Vander Heiden, 2009). In this process, anaerobic glycolysis is upregulated (this includes LDH, GAPDH, and PK enzymes). Hypoxia-

inducible transcription factor (HIF-1) becomes stabilized under hypoxic conditions and binds to DNA, inducing transcription of the major glycolytic genes. To allow for continuous glycolytic function, LDH regenerates the cofactor nicotinamide adenine dinucleotide (NAD⁺) through a process called lactic acid fermentation (Kim, 2005).

In Alzheimer's disease, a similar outcome occurs when the accumulation of plaques in the brain causes increased oxidative stress and subsequent damage to neuronal mitochondria (Whiteman et. al., 2005). Successful energy production depends on the upregulation of the glycolytic pathway since damaged mitochondria cannot effectively sustain mitochondrial respiration. Again, the upregulation of LDH is necessary to regenerate NAD⁺.

Figure 1: Energy production via anaerobic glycolysis versus via cellular respiration



Although oxidative phosphorylation produces more ATP than glycolysis, ROS damage to the mitochondria, and/or a lack of oxygen, can induce the cell to rely more heavily on glycolysis (located in the cytosol). The Warburg Effect in hypoxic tumor environments exemplifies this shift (Vander Heiden, 2009). (Image from Vander Heiden, 2009).

The goal of this research was to characterize how oxidative agents damage LDH – specifically how LDH’s five cysteine residues can be modified by biologically relevant oxidants like hypochlorous acid (HOCl), and how these modifications affect protein activity and conformation. We hypothesized that damaging oxidative agents like HOCl and oxidized phenolic compounds would modify LDH cysteine residues and negatively affect LDH activity. By exploring the extent to which different compounds interact with LDH, the enzyme’s behavior could be characterized, *in vitro*, using simulated disease environments. We were able to determine if damage we caused to the enzyme could be reversed, as well as whether we could protect the protein from the damaging agents prior to exposure.

There is still no cure for most neurodegenerative diseases, and there is no comprehensive understanding of ageing. By examining proteins that are conserved across cell types and that play important roles in metabolism – especially during times of cellular stress – scientists can further elucidate how these proteins function in disease states. The results of these experiments are useful in that they add to the knowledge scientists have been building regarding diseases of aging, showing how lactate dehydrogenase responds in AD conditions, and how key model proteins can be affected negatively by the products of antioxidant processes.

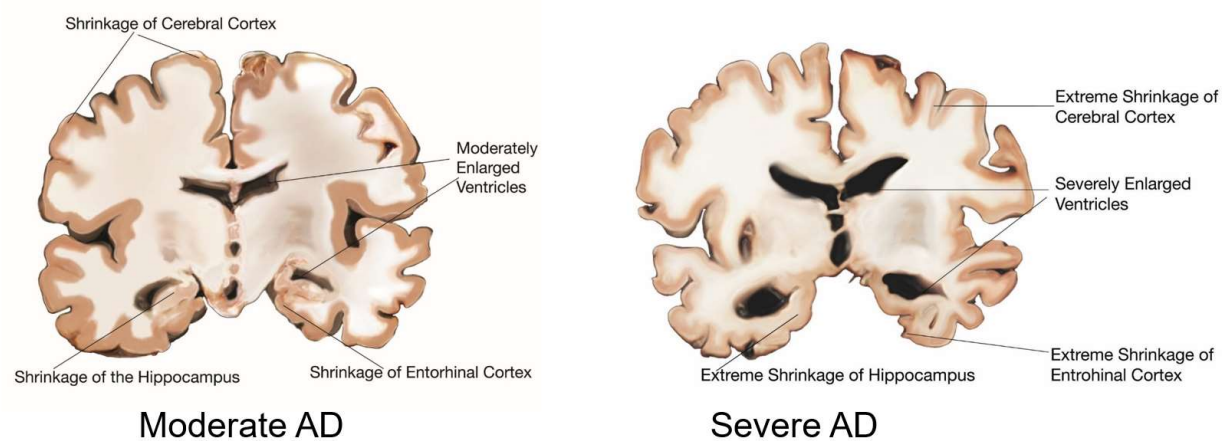
BACKGROUND

The background of this paper will focus on the relevance of this research to Alzheimer's disease, reactive oxygen species and antioxidants, the function of anaerobic glycolysis in disease states, lactate dehydrogenase's structure and function, the importance of thiol biochemistry and redox regulation in mammalian cells, and the three types of reactions this research is primarily concerned with: HOCl modification of cysteine residues, glutathione competition for reactive oxygen species, and modification of cysteine residues via quinone chemistry.

Alzheimer's disease pathology

Alzheimer's disease (AD) is a neurodegenerative brain disorder characterized by extracellular amyloid beta ($A\beta$) plaques and intracellular neurofibrillary tangles (Alzheimer's Association, 2016). Early symptoms of AD include memory loss, inability to perform daily tasks, and difficulty communicating. As AD progresses through the brain, patients experience personality changes, delusions, hallucinations, loss of muscle control, and eventual death. Currently, there is no cure for AD. It is the sixth leading cause of death in America, and in 2016, the costs associated with AD care were \$236 billion (Alzheimer's Association, 2016). Further research into AD mechanisms is imperative for mitigating the effects of this disease.

Figure 2: AD Progression from Moderate AD to Severe AD in Brain Cross-Section (National Institute on Ageing)



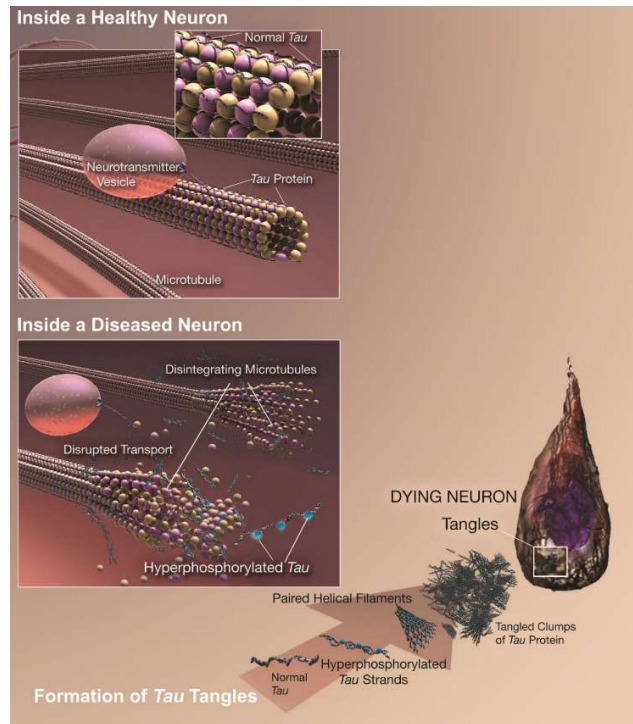
Over time, neurons affected by AD become isolated and unable to communicate with surrounding cells. This results in significant shrinkage of key brain areas such as the hippocampus and cerebral cortex. (Image from the National Institute on Aging).

Although research has successfully elucidated important elements of AD progression, no comprehensive description of an AD mechanism exists. The abnormal regulation of glycolysis in AD may play a key role in AD progression. Knowledge of this could help connect current AD research on oxidative stress, plaques, and neuron death.

Neurofibrillary Tangles and AD

Neurofibrillary tangles are insoluble, twisted fibers consisting of tau protein (Iba, 2013). They are found in the neurons of AD patients. In a normal brain, tau is a component of microtubules, an important structural protein in cells. In an AD brain state, abnormal tau causes the microtubules to collapse and aggregate. Although researchers do not know if these tangles are a result of AD conditions, or a cause of AD conditions, they are present in the brains of AD patients.

Figure 3: Neurofibrillary Tangles (Healthy vs. Diseased Brain) (National Institutes of Ageing)



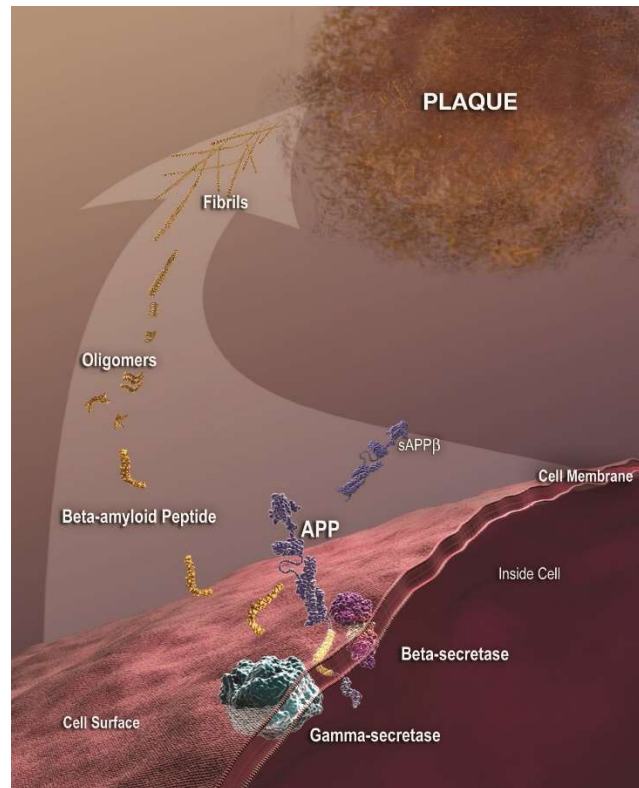
Neurofibrillary tangles occur within neurons when microtubules disintegrate, aggregate, and become insoluble tangles. These tangles disrupt cellular functions. (Image from the National Institute on Aging).

Amyloid Beta (A β) Peptides Form A β Plaques

A β plaques are insoluble accumulations of β -amyloid protein between neurons, and are a characteristic of AD patients' brains (Vlassenko, 2014). β -amyloid peptide fragments originate from a larger transmembrane amyloid precursor protein (APP). In normal brains, APP is broken down by gamma secretase, a protease specialized for cleaving single-pass transmembrane proteins. After cleavage, the short peptides are eliminated from the cell. In AD brains, APP is improperly broken apart due to mutated gamma secretases that cleave a shorter peptide from APP. The most common isoform

of gamma secretase is A β 40, but A β 42 leads to misfolding of A β cleaved peptides. This misfolding, in turn, leads to A β plaques. The accumulations of A β plaques can occur between 10 to 15 years prior to the onset of recognizable AD symptoms and AD diagnosis.

Figure 4: Formation of A β Plaques in AD (National Institute of Ageing)



The cleavage of APP plays an important role in formation of amyloid plaques in the brain (Vlassenko, 2014). (Image from the National Institute on Aging).

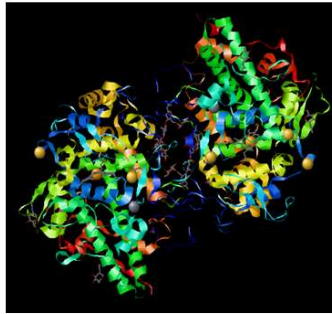
Reactive oxygen species (ROS) are chemically reactive compounds containing oxygen (Whiteman et. al., 2005). These species include peroxides, superoxides, hydroxyl radicals, and singlet oxygen molecules. ROS are a natural product of cellular metabolism and have roles in signaling and homeostasis (Espinosa-Diez et. al., 2015). However, when environmental stressors trigger large increases in ROS, the cell often

cannot respond quickly enough and ROS-induced damage to cellular structures occurs. At a high enough level, ROS can induce cell death (Whiteman et. al., 2005).

In a normal brain, ROS scavenging enzymes (e.g. glutathione) reduce damage from free radicals (Yap, 2006). In an AD brain, ROS is able to overwhelm these repair processes (Whiteman et. al., 2005). This excess of ROS damages the mitochondria. In turn, because the mitochondria are damaged, they produce more ROS due to the inability to fully reduce an oxygen molecule in the last step of oxidative phosphorylation due to malfunctioning electron transport chains. This creates a cyclic process that generates large amounts of ROS in the cell. In AD brains, molecular oxygen and ROS generated by malfunctioning mitochondria are trapped by A β plaques. Another enzyme, myeloperoxidase (MPO) also co-localizes with A β plaques and expression of MPO is elevated in neurons of AD brains (Green, 2004). In AD, MPO levels are elevated three-fold (Whiteman et. al., 2005). MPO converts trapped hydrogen peroxide (a type of ROS) to hypochlorous acid, HOCl. Because MPO levels are elevated, and there is a plethora of hydrogen peroxide available at plaque sites, HOCl levels are elevated as well, causing damage to cellular structures and disrupting metabolic processes. HOCl was significantly elevated in AD brain neurons indirectly using a chlorotyrosine biomarker only present when HOCl is also present in the cell (Dalle-Donne, 2006). HOCl induces apoptotic necrosis in cultured cortical neurons in a dose-dependent fashion (Yap, 2006).

Figure 5: MPO Structure and Reaction

Image created using RasMol and PDB protein ID 5FIW (Human MPO)



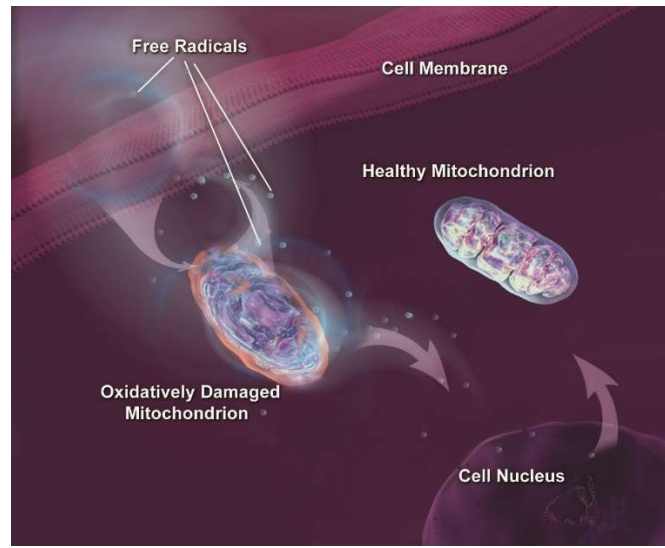
MPO converts hydrogen peroxide into HOCl. Both MPO and HOCl levels are elevated in AD.

Antioxidants: scavengers of ROS

Free Radicals

Free radicals are highly reactive unpaired electrons. Reactions with free radicals can include the propagation of unpaired electrons to other molecules or reactive species (Carocho, 2013). Free radicals can be formed through natural cellular process such as mitochondrial metabolism, however, when they react with the wrong substrates they can cause damage to cellular structures and processes. There are environmental causes for the formation of free radicals as well, including x-rays, pollutants, drugs, pesticides, and cigarette smoke. As shown in the above section regarding AD, free radicals play important roles in disease states.

Figure 6: Mitochondria in healthy vs. ROS-damaged cells



During Alzheimer's disease, mitochondria near amyloid beta plaques are irreparably damaged by ROS. As a result, energy production in the damaged mitochondria falters (Whiteman et. al., 2005). (Image from the National Institute on Aging).

These roles extend beyond AD. Radical oxygen species are important in the pathology of cancers, Parkinson's disease, ALS, and general aging processes (Lobo, 2010). For this reason, many scientists have sought ways to limit damage from free radicals and radical oxygen species.

Antioxidants

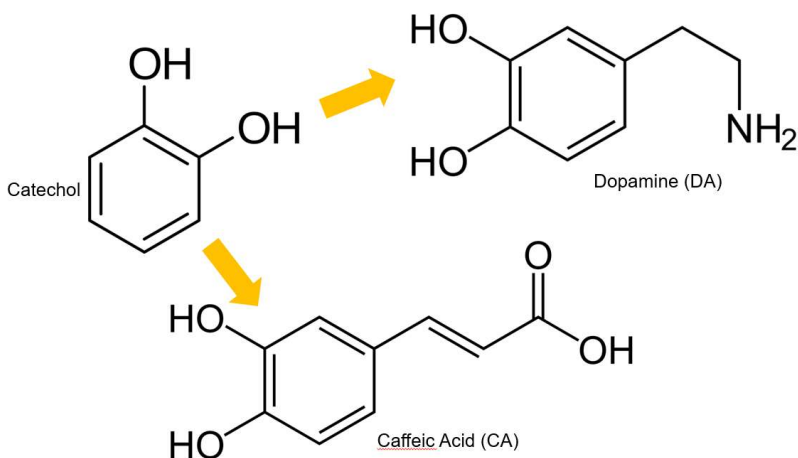
Antioxidants are compounds that can accept unpaired electrons, and thus stabilize radical species (Halliwell, 2008). They act to scavenge reactive radical species and thus shield the cell from damage to important cellular processes. Antioxidants act by two mechanisms. The first is through directly accepting unpaired electrons. Most antioxidant compounds have structures that allow them to remain stable despite accepting unpaired electrons (Carocho, 2013). The other method is indirect and

operates through inhibiting cellular processes that produce free radicals (Lu et. al., 2010). Antioxidants are found both in the body, produced through cellular processes, and in the food people consume regularly. Diets rich in fruits and vegetables have been linked to a decreased risk of getting AD and healthier aging (Pocernich et. al., 2011).

Ortho-phenols as antioxidants

Compounds with antioxidant properties include phenolic molecules that scavenge reactive oxygen species and prevent damage to the cell. These compounds are primarily derived from catechol, a compound commonly found in plants (Bolton et. al., 2017). Catechol-based compounds have a motif of two hydroxyl groups positioned ortho to one another on a benzene ring. Compounds like dopamine and caffeic acid have similar backbone structures, and are thus considered catechol-based derivatives.

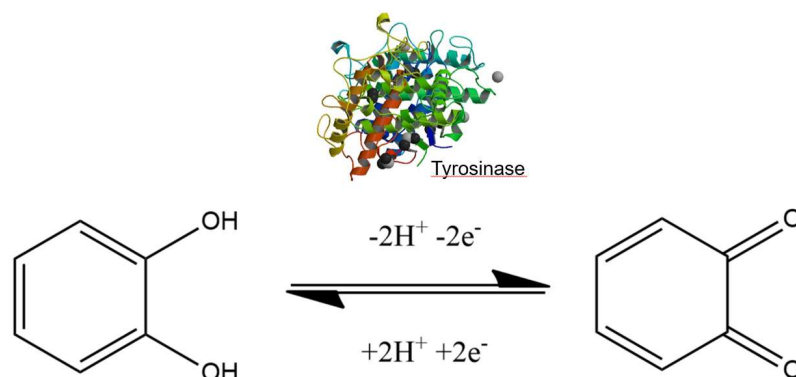
Figure 7: Examples of common ortho-phenolic catechol-derived antioxidants



Catechol-based ortho phenols all have a benzene ring structure with two hydroxyl groups attached in ortho positions. Structures created with ChemDraw.

In the reactive species scavenging process, catechol-based ortho-phenols can be oxidized to ortho-quinones.

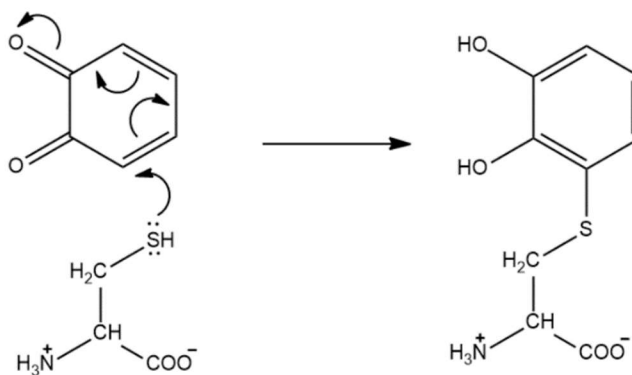
Figure 8: Oxidation of catechol to an ortho-quinone via tyrosinase



The mushroom tyrosinase enzyme was rendered in RasMol using the PDB file 3NM8. In this reaction, catechol is oxidized to benzoquinone. Image created with ChemDraw.

In turn, an ortho-quinone can undergo an irreversible Michael addition with thiol groups in the cell, including cysteine residues in proteins.

Figure 9: Cysteine modification by an ortho-quinone via Michael addition



An available cysteine on a protein can react easily with most ortho-quinones. The thiol group acts as a nucleophile and in the reaction process the quinone is reduced back to a phenol. Image created with ChemDraw.

This demonstrates the possibility for a compound with antioxidant properties to be converted into a pro-oxidant that can potentially damage proteins by binding to cysteine

residues. By modifying cysteine residues, ortho-quinones could disrupt both protein structure and function.

Energy production in disease states

Anaerobic Glycolysis

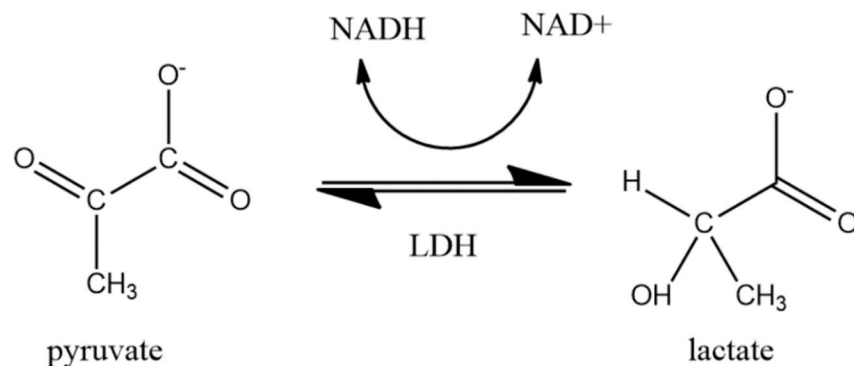
Reactive oxygen species in AD and cancers target mitochondrial respiration. To combat and prevent further damage to the mitochondria, diseased cells often upregulate glycolysis, a process that occurs in the cytosol of the cell, thus allowing for energy production without requiring functional mitochondrial respiration (Kim, 2005). Glycolysis consists of ten reactions that ultimately convert glucose to pyruvate and generate two net ATP molecules per each pyruvate produced from glucose. This is significantly less energy than the 32 molecules of ATP generated in mitochondrial respiration. Thus, to compensate for a loss of mitochondrial respiration, glycolysis must be significantly upregulated. When oxygen is not available (e.g. in tumor conditions), or the electron transport chain is malfunctioning, the cell may undergo lactic acid fermentation – the process by which energy is generated without the use of oxygen, also called anaerobic glycolysis. The upregulation of anaerobic glycolysis has been noted in cancers and in AD.

Recently, glycolytic enzymes have been implicated in pathways other than glycolysis (Kim, 2005). PK, LDH, GAPDH, and ENO1 all have dual roles as transcription factors. This recently discovered link between metabolic functions in the cytosol and transcription modifications in the nucleus demonstrate why it is important to continue to study glycolytic enzymes.

Lactate dehydrogenase (LDH) structure and function

LDH is responsible for conversion of pyruvate to lactate during anaerobic glycolysis (Kim, 2005). It facilitates the oxidation of the cofactor NADH to replenish NAD⁺. This process is key in disease states that depend on anaerobic glycolysis – without LDH and lactic acid fermentation, glycolysis would be unable to continue because NAD⁺ resources would deplete.

Figure 10: Lactate dehydrogenase replenishes NAD⁺ in anaerobic glycolysis

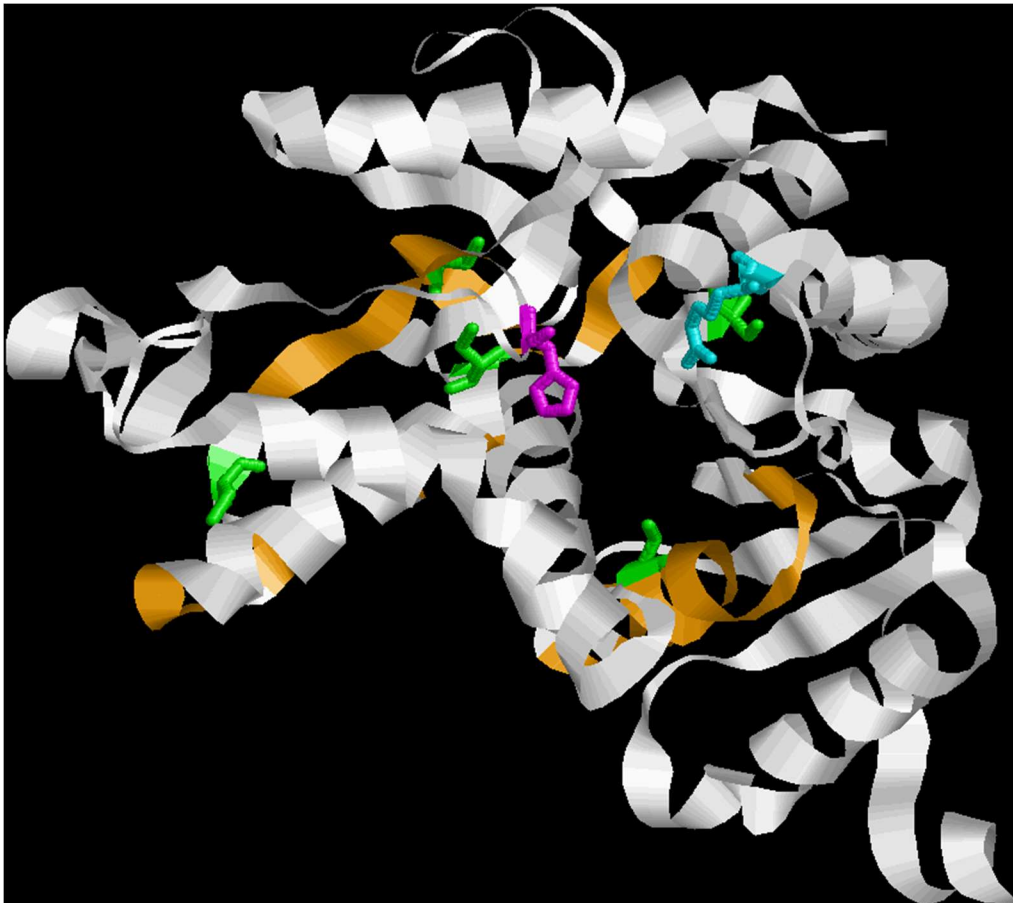


Anaerobic glycolysis, or lactic acid fermentation. Image created with ChemDraw.

LDH is composed of 4 subunits, each with catalytic capabilities (Diaz, 1993). One subunit has a mass of 36 kDa. Muscle LDH is encoded by the *LDH-A* gene. There is also an *LDH-B* gene that produces heart muscle LDH. A conserved catalytic histidine in the active site of the enzyme (histidine 192 in rabbit muscle LDH) helps to bind pyruvate following formation of the LDH/NADH complex (McClendon, 2005). If this histidine is modified before substrate binding, activity of the enzyme is greatly reduced. Arginine 109 (Arg111 in rabbit muscle LDH) plays an important role in solvating the carboxylic

acid group of the pyruvate and is part of approximately 10 amino acids that closes over pyruvate to secure its binding. Internally, LDH is highly hydrophobic and has an isoelectric point of 8.4.

Figure 11: Rabbit muscle LDH structure



Arginine 111 is in blue, histidine 192 is in magenta, cysteine residues are in green, and internal hydrophobic regions are highlighted in yellow. This image is directed into the open active site of LDH. Image created using RasMol and PDB file 3H3F.

LDH may also play important roles in other cellular functions (Kim, 2005). Lactate is an intercellular messenger, recruiting metabolic resources from astrocytes (Vlassenko, 2014). LDH also can act as a transcription factor such that when it is bound

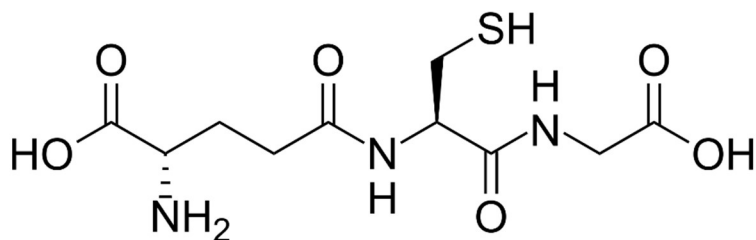
to DNA it enables the transcription of genes related to synaptic plasticity. LDH also has been implicated in other signaling mechanisms, including contributing to DNA helix destabilization (Kim, 2005). Because of LDH's many roles in the cell and its important role in energy production in disease states, studying LDH and its reaction to oxidative stress is imperative for furthering the understanding of disease mechanisms, and understanding the potential implications of damaged glycolytic enzymes on other aspects of cellular functions.

Protein thiol chemistry

Redox homeostasis

Endogenous thiols help to maintain redox homeostasis in cells (Lushchak, 2012). Low molecular weight thiols are ubiquitous in cells and include molecules like glutathione (GSH). These thiols scavenge reactive oxygen species, indirectly protecting proteins and other structures from damage. Thiols like glutathione can also interfere with protein structure and function by forming disulfide bridges with cysteine residues. Thus, it is important to maintain the right balance of free thiols in the cell such that they protect against free radical damage, but do not also disrupt cellular function. Glutathione is the most abundant free thiol in eukaryotic cells (Poole, 2015).

Figure 12: Glutathione structure



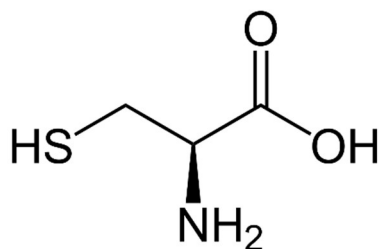
GSH is a common, highly abundant, substrate used for scavenging reactive oxygen species in cells. It also is used to maintain redox homeostasis in cells. Image created with ChemDraw.

Enzymes like superoxide dismutases scavenge radicals by converting superoxide anions to hydrogen peroxide and molecular oxygen. Enzymes like catalase, glutathione peroxidase, and peroxiredoxin then scavenge the hydrogen peroxide (Lushchak, 2012). Glutathione is used as a substrate for many of these reactions, and is thus found at concentrations ranging from 2 mM – 10 mM in the cytosol, mitochondria, nucleus, and endoplasmic reticulum.

Cysteine residues

Cysteine residues contain reactive thiols that often play key roles in protein structure and function; however, because of the reactive nature of cysteine residues, they are also often targets of oxidative stress and free radical damage (Giles et. al., 2003).

Figure 13: Cysteine amino acid structure



Cysteine is one of the twenty naturally occurring amino acids. Image created with ChemDraw.

Cysteine residues are highly nucleophilic both as S⁻ and as SH. They are also highly redox active with low redox potentials – this allows them to function as electron donors and facilitate electron transfer. Cysteine residues also can bind metals, as seen in alcohol dehydrogenase (ADH) where cysteine residues bind two catalytic zinc atoms. Thus, cysteine residues have the ideal properties to play important roles in catalysis in many proteins (Poole, 2015). It is important to study cysteine chemistry to further understand the role of cysteine residues in various enzymes and how different modifications of cysteine residues can affect enzyme function.

Thiol reactions investigated for this paper

HOCl, a relevant reactive oxygen species found in AD can react with cysteine residues in proteins to produce thiosulfinate, disulfides, and sulfenic acid (Hillion, 2015). Glutathione can both scavenge reactive oxygen species as well as bind directly to proteins or initiate disulfide bonds between two proteins. Ortho-quinones can covalently bond to cysteine residues via Michael addition.

Figure 14: LDH cysteine reactions with HOCl, GSH, and ortho-quinones

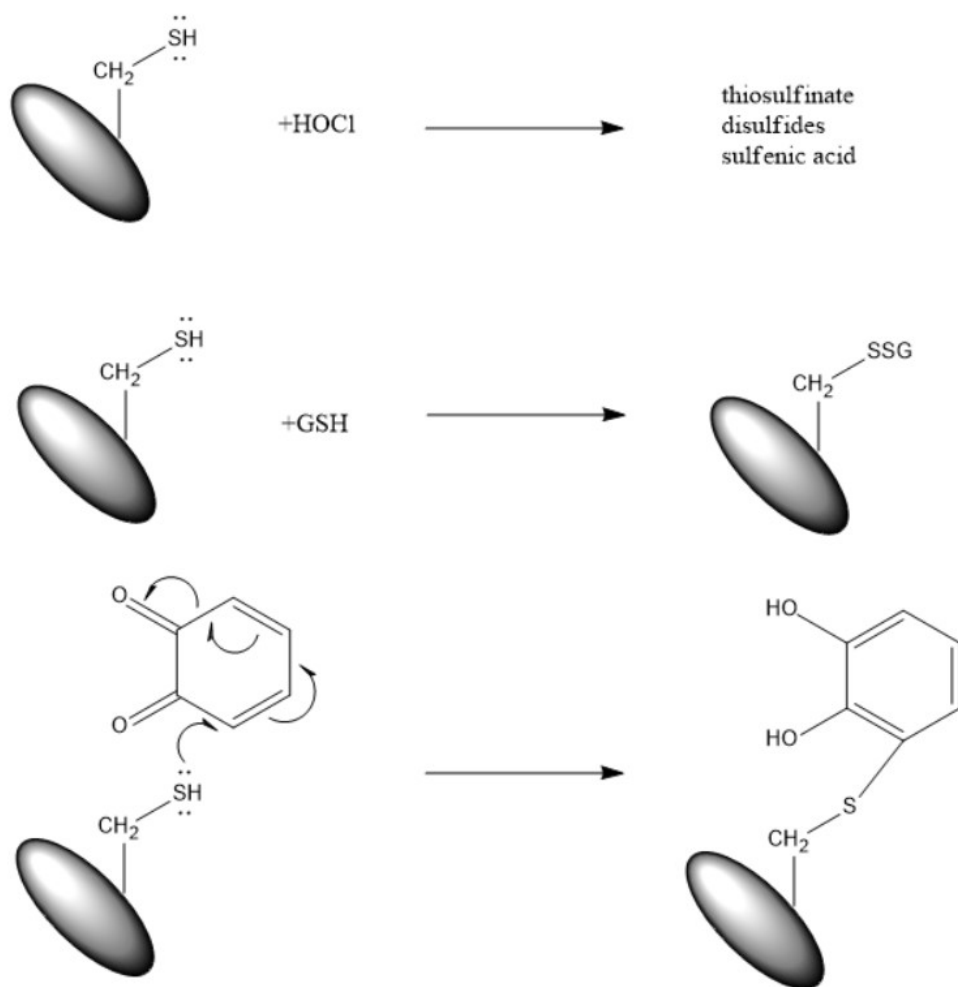


Image created with ChemDraw Ultra.

These are the reactions that will primarily be investigated in this paper.

Materials and Methodology

Materials

Purified proteins and cellular extracts:

Lactate dehydrogenase (LDH) from rabbit muscle (36,000 g/mol per subunit), alcohol dehydrogenase (ADH) from yeast (146,800 g/mol), and tyrosinase from mushroom were obtained from Sigma-Aldrich. Chicken muscle extract, chicken liver extract, and beef liver extract were produced from tissue samples obtained commercially. Yeast cell extract was produced from lysed yeast cells grown in lab by Dr. Lisa Landino.

Compounds:

HOCl, 5-(Iodoacetamido)fluorescein (IAF), 200 proof lab grade ethanol (EtOH), (tris(2-carboxyethyl)phosphine) (TCEP), nicotinamide adenine dinucleotide (NAD⁺), nicotinamide adenine dinucleotide + hydrogen (NADH), sodium pyruvate, catechol, PP60 tea extract, glutathione (GSH), and N-ethylmaleimide (NEM) were obtained from Sigma-Aldrich. Caffeic acid was obtained from Acros Organics. Ammonium persulfate and TEMED were obtained from Fisher Scientific.

Tea phenolic antioxidants were extracted in boiling water from Sigma Aldrich PP60 Green Tea Extract, Trader Joe's Organic Green Tea, Yogi Green Tea Kombucha, Clipper Rise & Shine, and Guayaki Yerba Mate Organic. Hops phenolic antioxidants were extracted from YCHHOPS German Hallertau hop pellets, YCHHOPS United States Cascade hop pellets, and LD Carlson's Apollo Hop Pellets.

Methods

For this research we conducted three major assays: an LDH kinetics assay using UV/Vis spectroscopy, an ADH kinetics assay using UV/Vis spectroscopy, and SDS-PAGE using oxidized LDH samples labeled with IAF.

Protein purification:

LDH from rabbit muscle was obtained in a suspension with 3.2 M ammonium sulfate (pH 7). Using a desalting column (Econo-Pac 10DG columns from Bio-Rad Laboratories in Munich, Germany) and buffer solution, the salt impurities in the original LDH suspension were removed. The concentrations of the purified LDH solutions were determined using UV/Vis spectroscopy and Beer's Law. Beer's Law relates Absorption (A) to the concentration of the sample in the following way:

$$A = \varepsilon * b * c$$

where ε is the extinction coefficient unique to the protein, b is the path length that the light travels through the sample, and c is the concentration of the protein in the sample (Powers et al., 2007). Absorption was read at 280 nm. The extinction coefficient for LDH is $176,220 \text{ cm}^{-1}\text{M}^{-1}$ (for one tetramer). The path length of the BioTek Instruments (Highland Park, Winooski, VT) microplate reader for the 96-well plate samples is 0.6 cm based on numerous calculations in lab.

ADH from yeast extract was obtained as a lyophilized powder. Using a desalting column, buffer salt impurities were removed. Purified ADH concentrations were determined using UV/Vis spectroscopy and Beer's Law. Absorption was read at 280 nm. The extinction coefficient for ADH is $189,320 \text{ cm}^{-1}\text{M}^{-1}$.

Preparation of chicken muscle, chicken liver, and beef liver extracts:

25 g of chicken muscle (or chicken liver or beef liver) was chopped into fine pieces, and suspended in 3 volumes (75 mL) of cold LDH extraction buffer composed of 20 mM Tris-HCl (pH 8.6) containing 1 mM DTT (a disulfide reducing agent). Tissue samples were then homogenized in a Waring blender for 2 minutes. Proteins were extracted by stirring for 1 hour at 4°C. The extract was centrifuged at 10,000 rpm for 45 minutes, prior to decanting the supernatant into a clean centrifuge tube. The supernatant was then centrifuged for the same time and speed. The final supernatant obtained after centrifuging was the final “extract.”

Preparation of tea and hops extracts:

One gram (or close to – see Appendix 3 for specific values) of each tea sample and each hops sample was dissolved separately in 100 mL of DI water and boiled for 30 minutes. The mixtures were filtered into sterile 50 mL test tubes. Aliquots from these 50 mL tubes were added to 1.5 mL centrifuge tubes and centrifuged for 15 minutes at 10,000 rpm. The supernatant was removed and added to new 1.5 mL tubes and these tubes were frozen at -20°C.

Oxidation of LDH and ADH samples:

2.36 mg/mL (65.2 μ M tetramer) LDH in 10 mM phosphate buffer (pH 7.4) and 2.43 mg/mL (66.21 μ M tetramer) ADH in 10mM phosphate buffer (pH 7.4) were stored at -80°C. After thawing, 2.29 μ L and 1.5 μ L of the respective LDH and ADH solutions were added to separate 0.5 mL microfuge tubes. Next, 10 mM phosphate buffer (pH 7.4) was added to the microfuge tubes in the desired amount, leaving room for an oxidizing agent or other modifying compound (eventually giving a total volume of 15 μ L

in the microfuge tube). Next, 1.5 μL of a desired concentration of an oxidizing agent (HOCl, caffeic acid, catechol, PP60, tea extract, or hops extract) was added to each microfuge tube. All of these oxidants were diluted in warm DI water with the exception of caffeic acid which was initially diluted in DMF, but can also be diluted in hot DI water). Lastly, 2.0 μL of 0.5 mg/mL tyrosinase was added if required (to catalyze the transition between ortho-phenolic compounds and ortho-quinones). The final concentration of cysteine amino acids in the microfuge tubes was 50 μM . Samples were incubated at 37°C for 30 minutes.

Modifications of oxidation process:

Following sample incubation at 37°C, 2.0 μL of 5.0 mM TCEP (a reducing agent) could be added to the samples to determine if any oxidation damage could be reversed. Control samples received 2.0 μL of DI water. Samples were incubated a second time, for 5 minutes.

Prior to incubation (included in 15 μL of total sample volume) and to oxidant addition, glutathione dissolved in DI water could be added to the LDH and ADH samples. The samples were then incubated for the usual 30 minutes at 37°C.

For assays involving pH variation, the samples were prepared in 10 mM phosphate buffer (pH 6.0, 6.4, 6.9, 7.4, and 8.0).

LDH kinetics procedure:

Using a BioTek Instruments microplate-reader, transparent Corning 96-well plates, and Gen5 Version 1.11 (2005 BioTek Instruments) UV/Vis analysis software, LDH activity was determined based on the oxidation of NADH (absorbance at 340 nm) to NAD^+ (no absorbance at 340 nm).

First, following incubation, the oxidized LDH was diluted 1:50 in 10 mM phosphate buffer (pH 7.4 unless pH variation was being tested in which case the pH of the dilution matched the pH of the initial sample).

Then, in a 96-well plate, the following was prepared:

	Column 1: Blank	Column 2: Assay Control	Column 3: Sample #1	Column 4-12: Samples #2-10
Row A	200 μ L 10 mM Tris buffer (pH 7.4)	190 μ L 10 mM Tris buffer (pH 7.4) 10 μ L 10mM NADH	160 μ L 10 mM Tris buffer (pH 7.4) 15 μ L 10 mM pyruvate 15 μ L of 1:50 diluted sample #1 10 μ L 10 mM NADH	160 μ L 10 mM Tris buffer (pH 7.4) 15 μ L 10 mM pyruvate 15 μ L of 1:50 diluted sample N 10 μ L 10 mM NADH

After the addition of the NADH, the individual wells were mixed three times quickly with a 200 μ L pipette and the plate inserted into the reader. The reader was kept at 37°C. Absorbance of NADH was read every 30 seconds for 5 minutes at 340 nm. Using Beer's Law and linear regression, a rate in mM NADH/min/mg LDH could be determined. The extinction coefficient for NADH is 6220 M⁻¹cm⁻¹ (Bergemeyer, 1975). The calculated pathlength was 0.6 cm.

ADH kinetics procedure:

Using a BioTek Instruments microplate-reader, transparent Corning 96-well plates, and Gen5 Version 1.11 (2005 BioTek Instruments) UV/Vis analysis software,

ADH activity was determined based on the reduction of NAD⁺ (no absorbance at 340 nm) to NADH (absorbance at 340 nm).

First, following incubation, the oxidized ADH was diluted 1:50 in 10 mM phosphate buffer (pH 7.4 unless pH variation was being tested in which case the pH of the dilution matched the pH of the initial sample).

Then, in a 96-well plate, the following was prepared:

	Column 1: Blank	Column 2: Assay Control	Column 3: Sample #1	Column 4-12: Samples #2-10
Row A	200 μ L 20 mM Tris buffer (pH 8.8)	185 μ L 20 mM Tris buffer (pH 8.8) 10 μ L 10 mM NAD ⁺	155 μ L 20 mM Tris buffer (pH 8.8) 15 μ L 1 M EtOH 15 μ L of 1:50 diluted sample 1 15 μ L 10 mM NAD ⁺	155 μ L 20 mM Tris buffer (pH 8.8) 15 μ L 1 M EtOH 15 μ L of 1:50 diluted sample N 15 μ L 10 mM NAD ⁺

After the addition of the NAD⁺, the individual wells were mixed and the plate inserted into the reader. The reader was kept at 37°C. Absorbance of NADH was read every 30 seconds for 5 minutes at 340 nm. Using Beer's Law and linear regression, a rate in mM NADH/min/mg ADH could be determined.

IAF labeling procedure and SDS-PAGE

Following sample incubation for 30 minutes, 2 μ L of 5.0 mM IAF was added to each sample. Samples were incubated for an additional 30 minutes. During sample incubation, a 10% separating gel was prepared using Mini-PROTEAN Tetra Cell

supplies (from Bio-Rad Laboratories in Munich, Germany), 4.0 mL of DI water, 3.33 mL of 30% acrylamide, and 2.5 mL of 1.5 M Tris Buffer (pH 8.8). After mixing, the solution was degassed for 5 minutes under vacuum. Next, 100 μ L of 10% SDS and 50 μ L of 10% ammonium persulfate were added to the solution. ~15 μ L of TEMED initiated gel polymerization in approximately 20-30 minutes.

After the separating gel polymerized, a stacking gel was prepared using 1.5 mL of DI water, 0.335 mL of 30% acrylamide, 0.625 mL of 0.5 M Tris buffer (pH 6.8), 50 μ L of 10% SDS, 50 μ L of saturated ammonium persulfate, and 5 μ L of TEMED. The stacking gel was layered on the separating gel and polymerized in approximately 20 minutes. Well combs were removed and wells were rinsed.

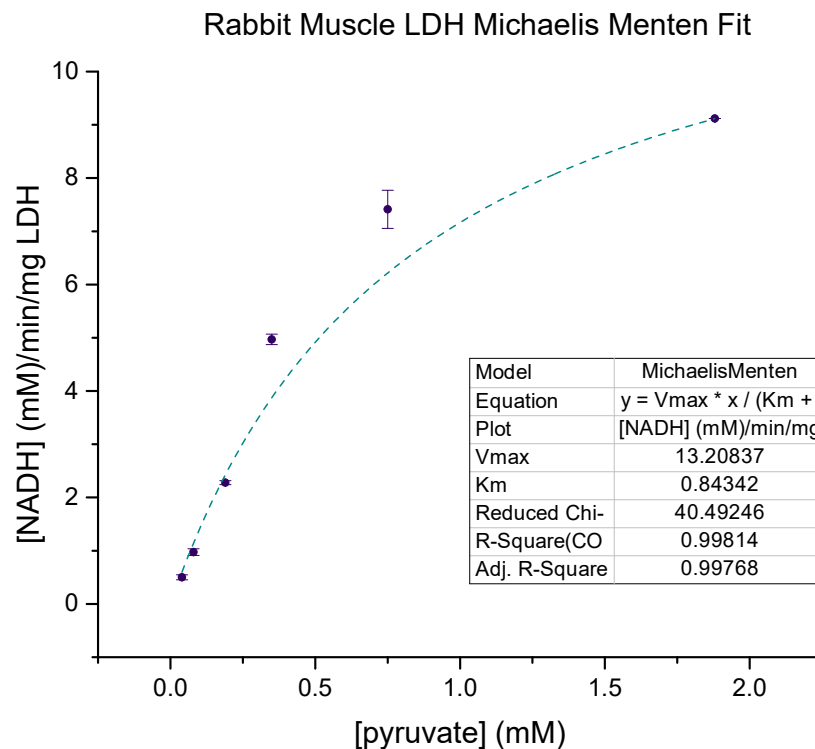
After samples incubated with IAF, sample buffer (+ BME) was added to each sample test tube. Samples were loaded into wells. Gels were run for approximately 1.5 hours at 90 volts. After electrophoresis was complete, gels were removed and imaged using a ChemiDoc XRS+ Imaging System (from Bio-Rad Laboratories in Munich, Germany).

RESULTS AND DISCUSSION

Rabbit muscle LDH kinetics

First, Vmax and Km values for the rabbit muscle LDH used in lab were determined by varying concentrations of pyruvate (substrate) while maintaining known concentrations of NADH (cofactor) and LDH. Reactions were run using the LDH kinetics procedure outlined in the methodology section; however, pyruvate concentrations ranged from ~0.05 mM to ~2.00 mM. The following Michaelis Menten fit was produced using OriginPro 2016 analysis software.

Figure 14: Michalis Menten Approximation for LDH Kinetic Activity



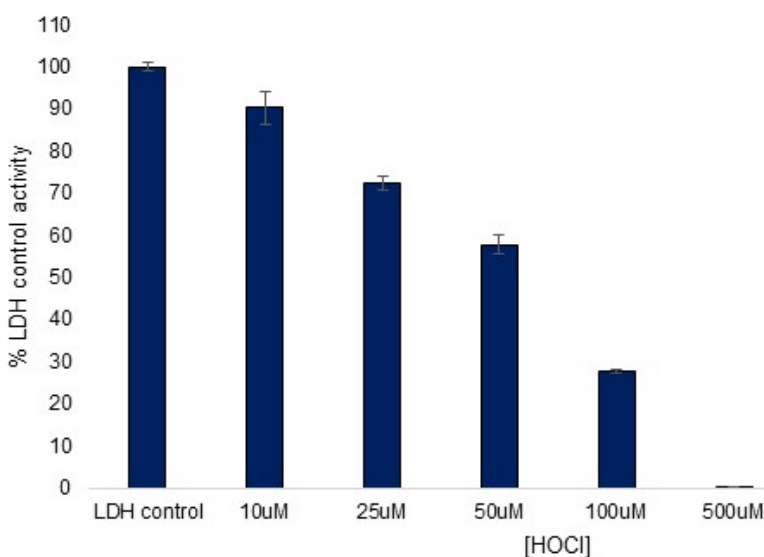
To establish this curve, a linear fit was applied to the initial reaction rates for LDH at each pyruvate concentration. The linear fits were determined across three trials and averaged (the error bars are very small, but present on the graph). Next, a Michaelis Menten curve fit was applied to the data using OriginPro 2016. Based on R values nearly equal to 1, the curve fit was satisfactory and Vmax and Km values for rabbit muscle LDH were reported.

The fit indicates a V_{max} value of 13.2 mM NADH consumed per minute per milligram of LDH. The K_m concentration was determined to be 0.8 mM of pyruvate. These values matched expected literature V_{max} and K_m values for rabbit muscle LDH (Hess, 1970). This information indicated that further experimentation on the rabbit muscle LDH enzyme could be done with confidence that the enzyme behaved as expected *in vitro*.

Rabbit muscle LDH and HOCl

Because of the relevance of hypochlorous acid (HOCl) in Alzheimer's disease, LDH was exposed to varying concentrations of HOCl to determine whether HOCl decreased LDH activity and modified cysteine residues on the protein. HOCl modification of LDH was then compared with modification of LDH by N-ethylmaleimide (NEM), a known thiol group modifier (Alexander, 1958).

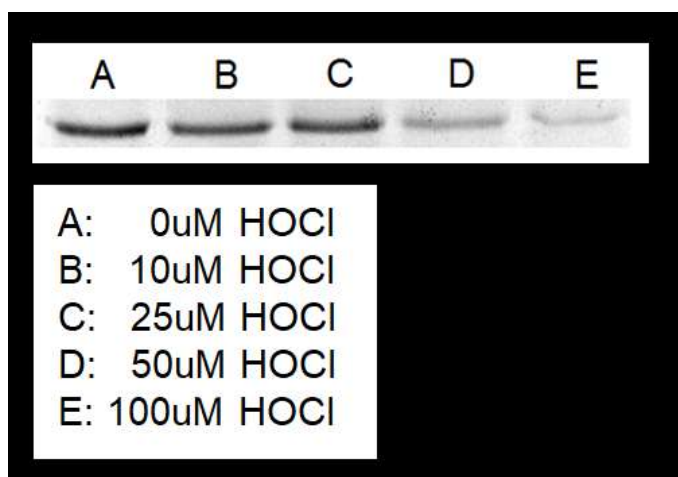
Figure 15: Inhibition of rabbit muscle LDH with HOCl



For each HOCl concentration, LDH was incubated with the oxidant for 30 minutes. The results were compared to a control sample without HOCl. The results were averaged over six trials.

Addition of HOCl at each concentration decreased LDH activity significantly ($p < 0.05$) compared with the control (using a one-way ANOVA test via OriginPro 2016). To determine if this decrease in activity correlated with cysteine modification, HOCl first was added to LDH samples. Then, after incubation, IAF was added. If the HOCl successfully modified the cysteine residues in LDH, we expected to see decreased labeling with IAF as HOCl concentrations increased, and did indeed observe these expected results.

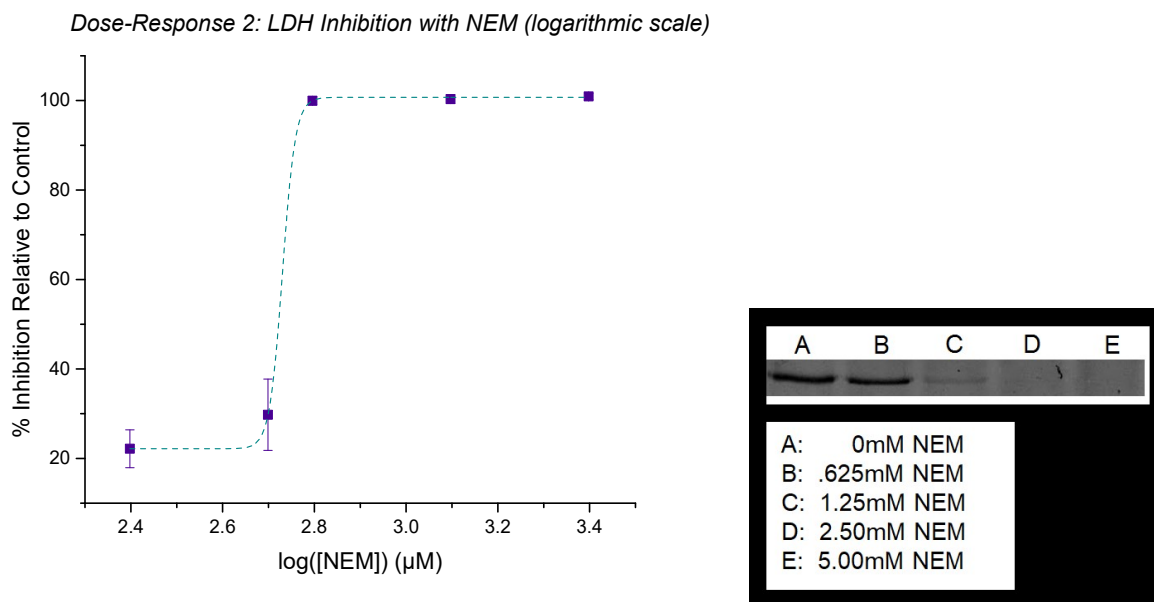
Figure 16: IAF labeling of rabbit muscle LDH after HOCl addition



Shown above is an inverted image. As HOCl concentrations increase, the fluorescence of the gel bands decreases. Because IAF modifies cysteine residues, we can confirm that as HOCl is added in increasing amounts to LDH, IAF molecules are unable to access as many cysteine residues.

To compare these results with a known cysteine modifier, varying concentrations of NEM were reacted with LDH causing a clear decline in enzyme activity, and IAF labeling confirmed that NEM modified LDH cysteine residues.

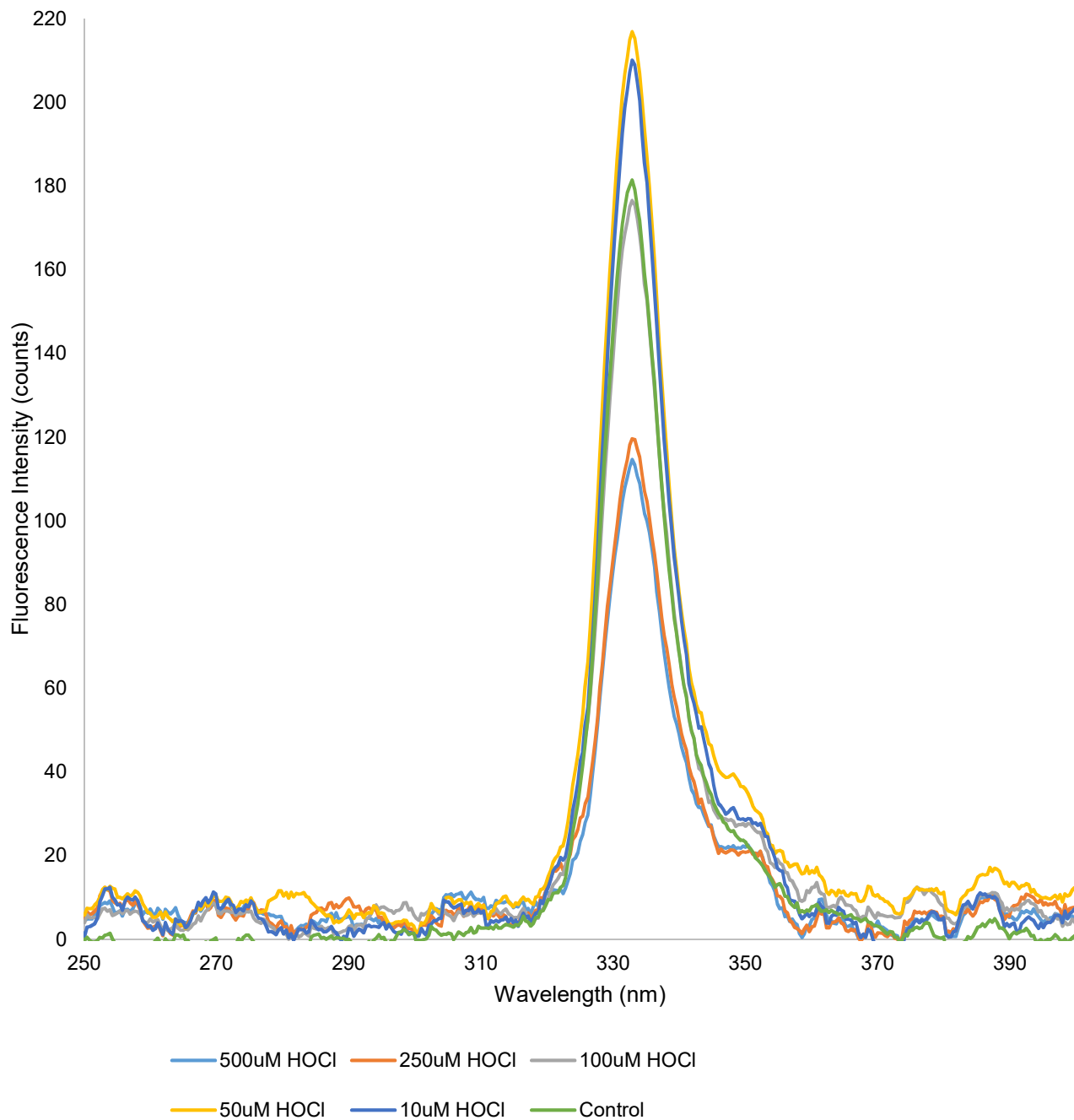
Figure 17: Inhibition of rabbit muscle LDH with NEM; IAF labeling of LDH after NEM addition



Using OriginPro 2016, a dose-response logarithmic curve was established for LDH inhibition with NEM. NEM inhibits LDH across the range of concentrations shown on the gel and IAF labeling of cysteine residues decreases as NEM concentration increases.

In conclusion, addition of HOCl at concentrations as low as 25 µM to 50 µM samples of LDH inhibited LDH activity and modified cysteine residues on the protein or changed protein conformation such that IAF could not label all of the LDH cysteine residues. Additional analysis of tryptophan fluorescence in LDH shows that as HOCl is added to LDH samples, tryptophan fluorescence changes. There is a tryptophan at position 187 in rabbit muscle LDH (using the PDB 3H3F file) which is very close to a cysteine residue at position 184. If Cys184 is modified by HOCl and conformation around that residue changes, there could be significant changes in the nearby tryptophan fluorescence.

Figure 18: Tryptophan (W) fluorescence in rabbit muscle LDH with addition of HOCl



As HOCl was added to LDH samples, the tryptophan fluorescence at 340 nm changed in intensity. At low concentrations of HOCl (10-50 μM) following 30 minutes of incubation with oxidant, the tryptophan

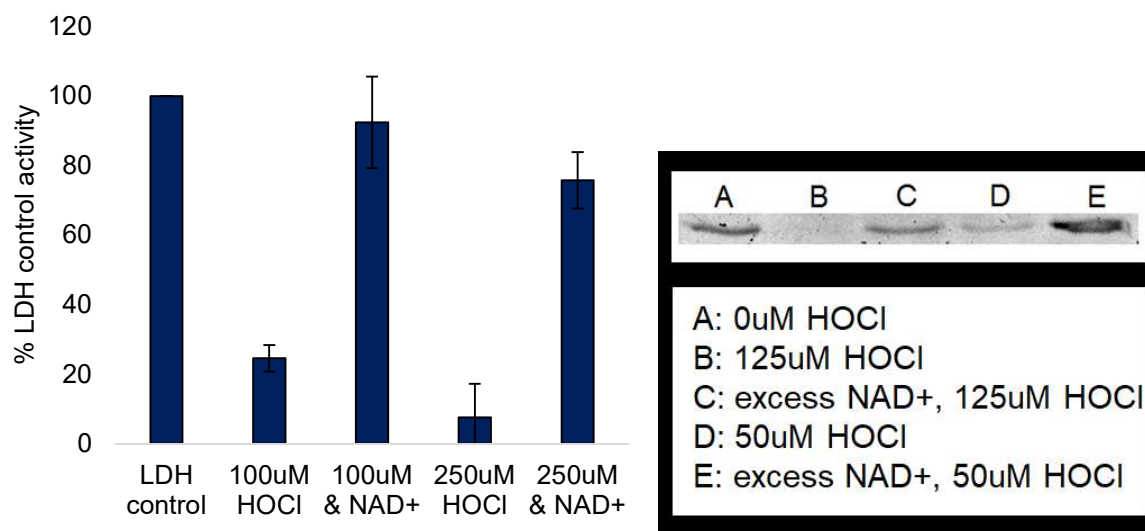
fluorescence increased. At higher concentrations of HOCl (100-500 μM), the tryptophan fluorescence intensity decreased.

Based on the results of the tryptophan fluorescence and the proximity of tryptophan 187 to cysteine 184, there are likely conformational changes that occur when LDH is exposed to concentrations of HOCl ranging from 10 μM to 500 μM . This further substantiates the claim that HOCl does modify cysteine residues on LDH since the fluorescence behavior of tryptophan 187 changes so significantly. Most likely, the environment around the tryptophan is changing as protein conformational shifts occur. This aspect of the project needs more investigation, and will be addressed further in subsequent months.

Protection of LDH from HOCl damage

Following confirmation that HOCl inhibits rabbit muscle LDH, NAD^+ was used to attempt to protect the protein from HOCl damage. NAD^+ was initially added to LDH. This solution was incubated for 5 minutes at 37°C. Then HOCl was added and the samples were incubated for the usual 30 minutes.

Figure 19: Protection of rabbit muscle LDH from HOCl oxidation by NAD⁺



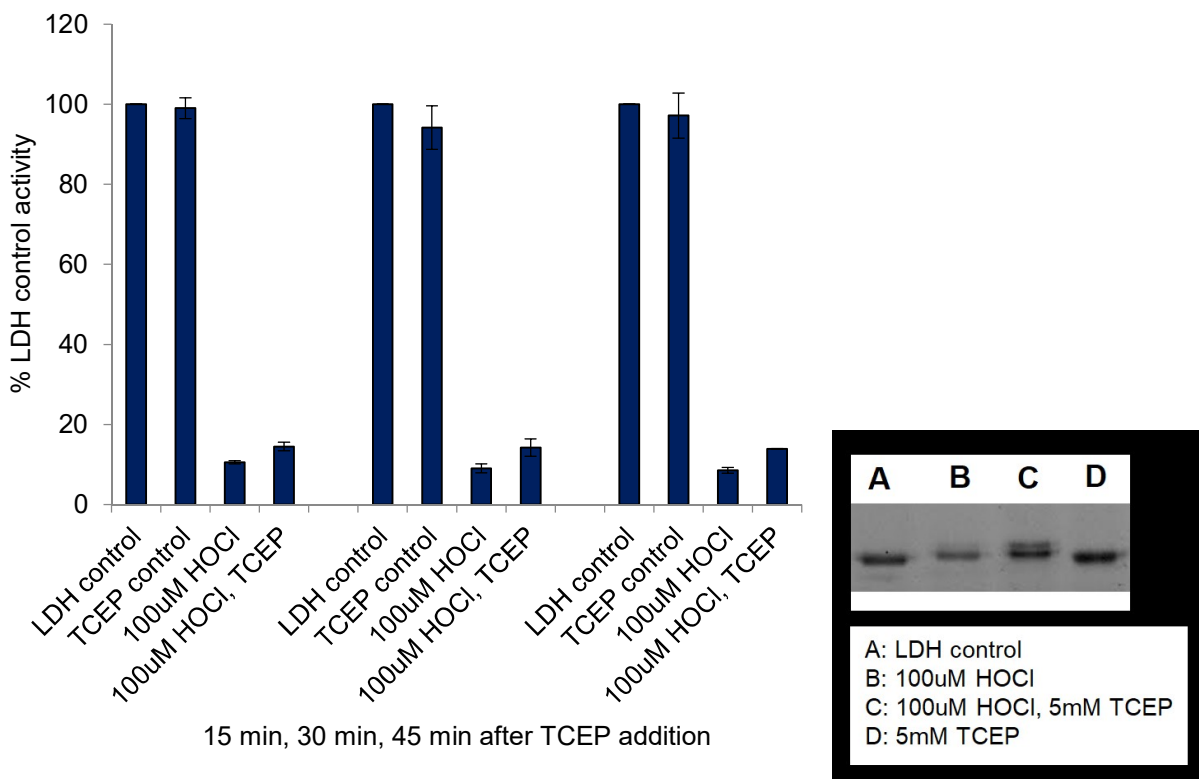
“C1” is the LDH control (-NAD⁺, -HOCl). When NAD⁺ is bound to rabbit muscle LDH prior to addition of HOCl, less damage occurs than predicted by HOCl addition with no protection. IAF labeling of cysteine residues remains intense (dark) when HOCl is added if NAD⁺ is first bound to the rabbit muscle LDH. HOCl does not react with NAD⁺ or NADH.

While protection with NAD⁺ and NADH successfully prevented activity decline, pyruvate did not have the same preventative effects. We attributed this to pyruvate’s smaller size relative to NAD⁺/NADH, as well as that the binding site for pyruvate is slightly different from the binding site for NAD⁺/NADH. Since NAD⁺/NADH is large, when it is bound it could be more effective at shielding the active site and internal cysteine residues from oxidative damage than pyruvate. In the case of LDH activity, NADH binding precedes substrate binding (Deng, 2001). Once NADH binds to LDH, the loop that facilitates binding of pyruvate is able to open and allow the substrate to fit into the active site (Pineda, 2007).

Reduction of oxidized LDH with TCEP

TCEP, a common reducing agent used in biochemical applications, was used to attempt to restore activity to HOCl-oxidized rabbit muscle LDH. LDH that had been incubated with HOCl for 30 minutes was exposed to 2.0 μL of 5 mM TCEP (for a concentration of $\sim 600 \mu\text{M}$ in the microfuge tube samples). This reaction was incubated for an additional 15, 30, and 45 minutes. While activity was not restored significantly, IAF labeling did increase.

Figure 20: Reduction of oxidized LDH with TCEP; activity and IAF labeling

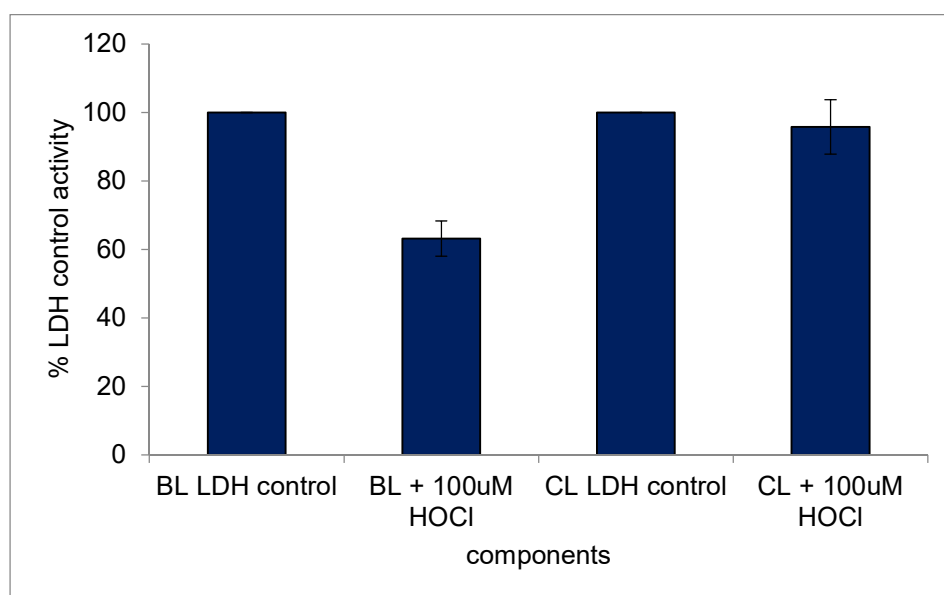


TCEP did not restore much activity to the rabbit muscle LDH; however, IAF bands appear to be darker when TCEP is added to the oxidized LDH sample. All experiments were performed three times and averaged.

Oxidation of LDH with HOCl in chicken and beef liver extracts

To determine if LDH could be oxidized with HOCl in the context of a cellular extract, we exposed chicken and beef liver extracts to 100 μM of HOCl and ran the usual LDH kinetics procedure on the samples.

Figure 21: LDH activity and HOCl modification of LDH in Beef liver and chicken liver extracts



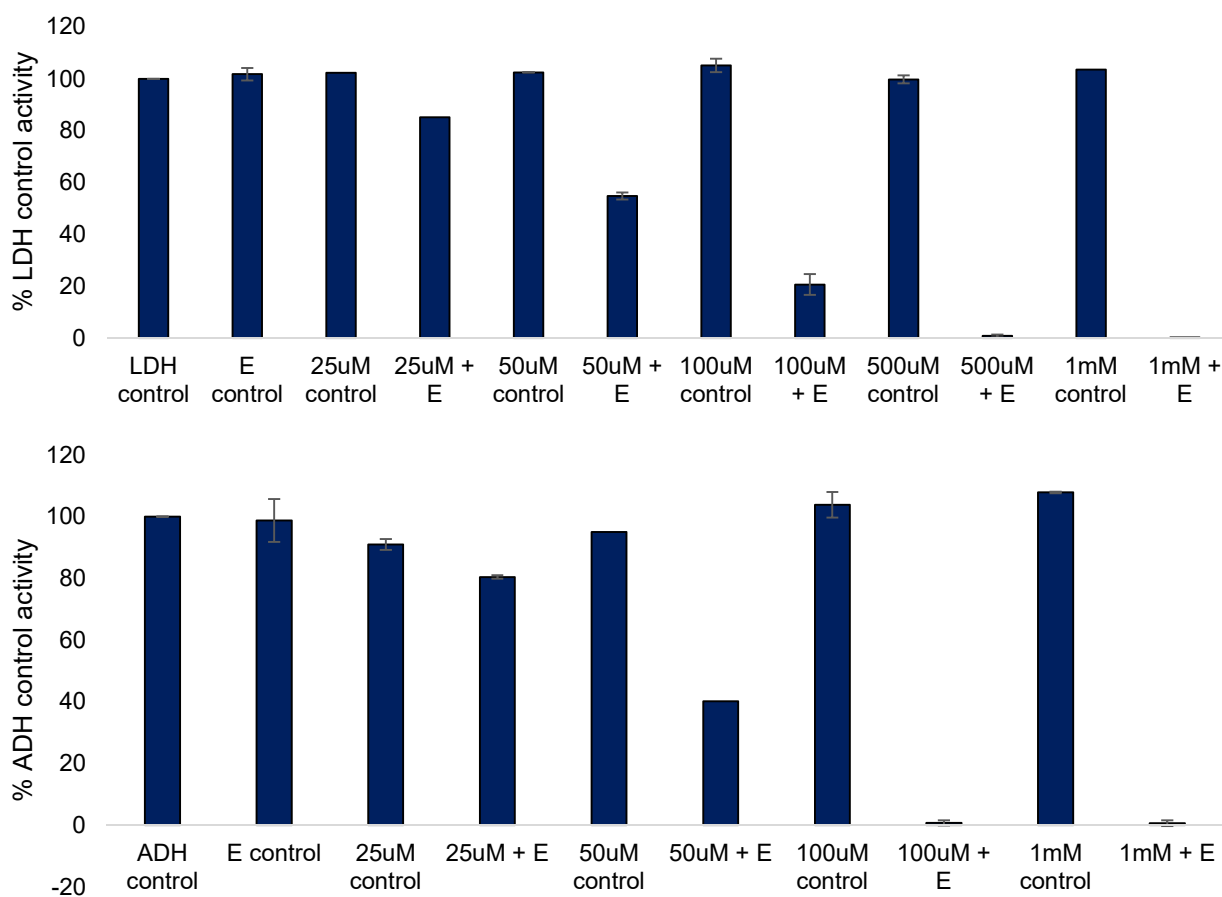
LDH activity was present in both the beef (BL) and chicken liver (CL) extracts. At 100 μM of HOCl, inhibition of LDH activity could be seen clearly in the beef liver extract. There was no significant change in LDH activity in the chicken liver extract.

Beef liver extract LDH showed a decrease in activity at 100 μM HOCl, but chicken liver LDH did not (even when higher concentrations of HOCl were added). This could be due to the abundance of other proteins that were reacting with the HOCl or scavengers in the extract – because of the desalting column, GSH and other small molecule thiols were removed.

Oxidation of LDH and ADH with ortho-quinones

To understand the extent to which oxidized catechol-based derivatives could modify LDH and change the protein's activity, phenolic compounds including catechol and caffeic acid, were oxidized to quinones using mushroom tyrosinase (E). The quinones were then added to solutions of LDH. First, catechol, a compound found in all plants was oxidized to its corresponding quinone and tested with LDH. We chose to compare our results to those using ADH from yeast, another protein with essential cysteine residues.

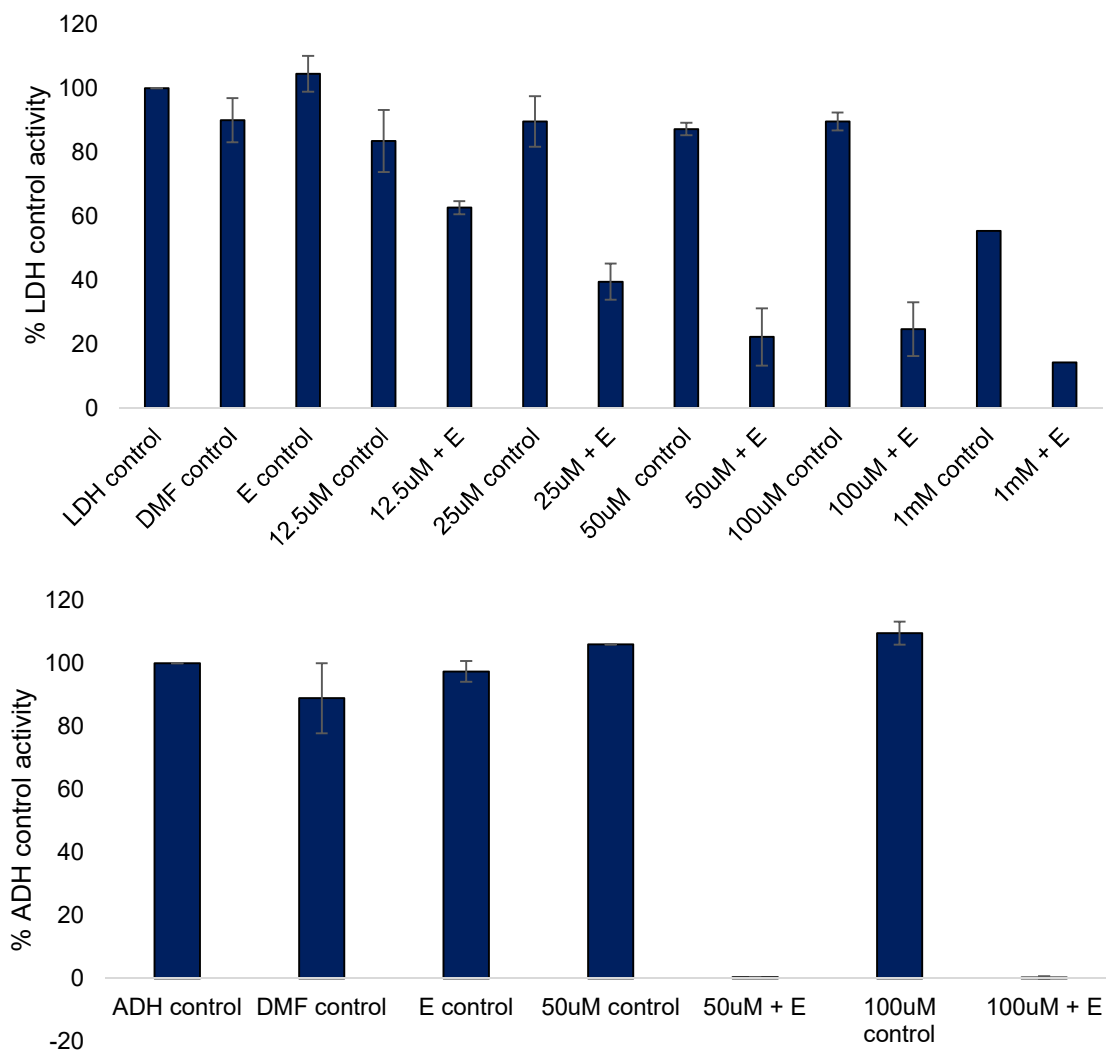
Figure 21: Oxidation of rabbit muscle LDH and yeast ADH with oxidized catechol (benzoquinone)



ADH and LDH assays were performed according to the procedures outlined in the methodology section. "E" refers to the tyrosinase enzyme. Shown above are averages across three trials.

Benzoquinone inhibits LDH and ADH activity starting at concentrations as low as 25 μM . Catechol does not. These results matched expectations since the mechanism for oxidation of protein cysteine residue by quinones follows a Michael addition, and thus the carbonyls on the conjugated ring are important for reaction with thiol groups on proteins (Bolton, 2017). Oxidized caffeic acid had similar effects on LDH and ADH activity.

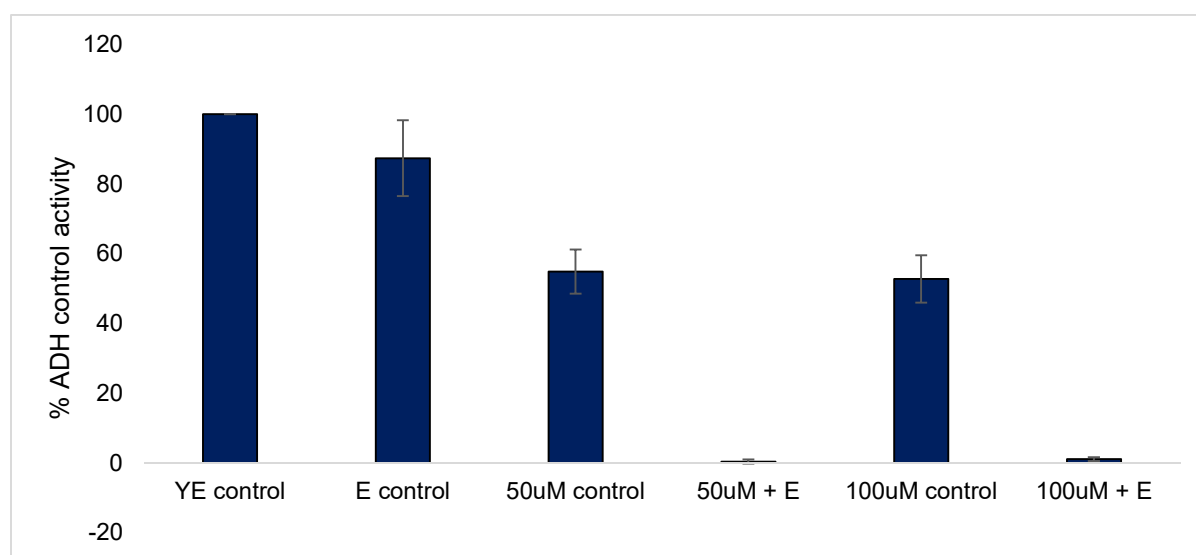
Figure 22: Oxidation of rabbit muscle LDH and yeast ADH with oxidized caffeic acid



ADH and LDH assays were performed according to the procedures outlined in the methodology section. "E" refers to the tyrosinase enzyme. Shown above are averages across three trials.

These results lead us to test oxidized catechol and caffeic acid on LDH and ADH in cell extracts. Chicken muscle extract was used to test for LDH inhibition with caffeic acid, and yeast cell extract was used to test for ADH inhibition. There was little to no effect on the LDH in the chicken extract, likely due to the many proteins that could have been oxidized instead of LDH. However, there was a decrease in ADH activity using the yeast extract.

Figure 23: Oxidation of ADH in yeast extract using oxidized caffeic acid



Yeast extract assays were performed according to the procedures outlined in the methodology section. “E” refers to the tyrosinase enzyme. “YE” refers to “Yeast Extract.” Data summaries shown above are averages across three trials.

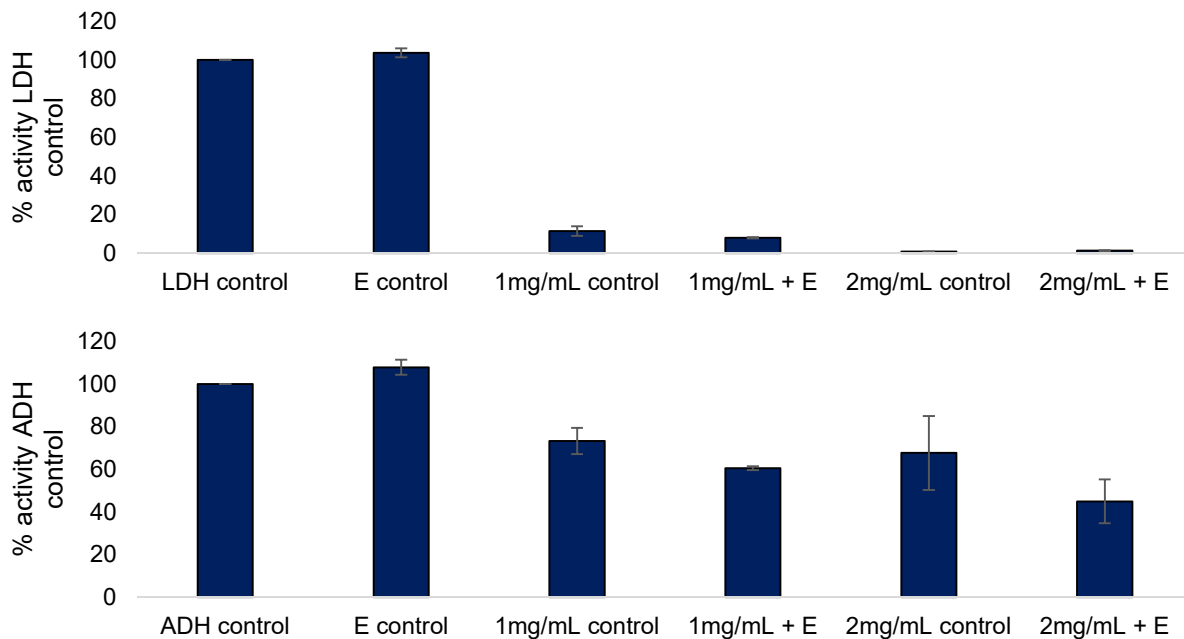
While it is clear that tyrosinase-oxidized caffeic acid significantly depleted ADH activity in the yeast extract samples, the control non-oxidized caffeic acid samples also showed decreased activity. This could be due to other processes occurring in the yeast extract that are capable of oxidizing caffeic acid, such as the presence of peroxidases. When hydrogen peroxide was added to yeast extract samples along with catechol but

no tyrosinase, more inhibition of ADH activity could be seen, giving some credence to this theory.

After examining the effects of oxidized catechol and caffeic acid on LDH and ADH activity, other phenolic derivatives were tested. This included oxidized dopamine, oxidized morin, oxidized alizarin, etc. (see Appendix 3). These compounds were selected to test the limit of how sterically hindering a compound could be before it no longer bound to LDH or ADH to inhibit activity, as well as how diverse the conjugated ring could be in terms of number of hydroxyl groups and location. The results of these studies are summarized in Appendix 3. We determined that many compounds larger than dopamine were not as potent, and compounds with more than two hydroxyl groups also did not inhibit the enzymes as well although this feature mattered less than size.

After looking at individual compounds, extracts from various teas and hops were tested for inhibitory properties. PP60 tea extract was purchased and tested first since it has known components.

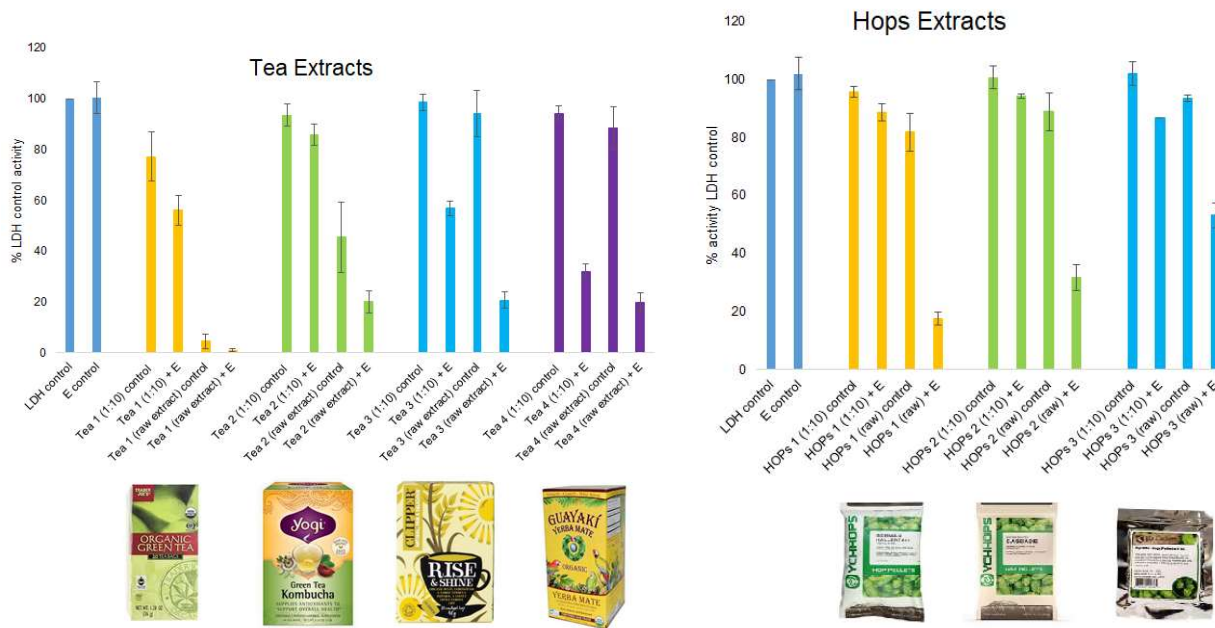
Figure 24: Oxidation of rabbit muscle LDH and yeast ADH with oxidized phenolic compounds in PP60 green tea extract



ADH and LDH assays were performed according to the procedures outlined in the methodology section. "E" refers to the tyrosinase enzyme. The PP60 extract was diluted to 1 mg/mL and 2 mg/mL in DI water. 1.5 μ L of these solutions were added to each sample of protein and then incubated. Shown above are averages across three trials. The extract contains 60% catechin, 34% (-)-epigallocatechin-3-gallate, 16.7% (-)-epigallocatechin, 8.7% (-)-epicatechin-3-gallate, 7.3% (-)-epicatechin, 2.8% (-)-gallocatechin gallate, and 0.5% (-)-catechin gallate, tannic acid, or (-)-epigallocatechin-3-gallate.

Once it was determined that PP60 green tea extract inhibited LDH and ADH activity, extracts were obtained from four different teas (two green, two herbal), and three hops varieties. LDH and ADH were exposed to these extracts using the standard oxidation process outlined in the methodology section. The most significant effects occurred with LDH.

Figure 25: Oxidation of rabbit muscle LDH with oxidized phenolic compounds in tea extracts and hops extracts



The tea extracts were from (left to right): Trader Joe's Organic Green Tea, Yogi's Green Tea Kombucha, Clipper's Rise and Shine Herbal Tea, and Guayaki Herba Mate Herbal Tea. The hops extracts were from (left to right) YCHHOPS German Hallertau, YCHHOPS United States Cascade, and LD Carlson's Apollo hops pellets. A 1:10 dilution of the extracts was made and both the dilution and raw extracts were tested with LDH. "E" stands for "tyrosinase enzyme."

The tea and hops extracts that were combined with tyrosinase all inhibited LDH activity. There was, however, a difference between the herbal teas and the green teas. The green teas clearly inhibited LDH activity with and without the tyrosinase addition, behaving like the PP60 green tea extract. The herbal teas only inhibited LDH with the addition of tyrosinase. The hops extracts behaved this way as well. Our lab still needs to perform LC/MS on the extracts to determine their exact compositions, but we know that these extracts contain at least catechol since catechol is an essential component of all plant cell walls.

Glutathione competition with oxidants

Glutathione (GSH) was added to ADH and LDH samples prior to addition of HOCl and caffeic acid. The samples were incubated for the usual 30 minutes. Results indicated that for both ADH and LDH (and for both oxidants), GSH at concentrations ranging from 2 mM to 10 mM successfully scavenged oxidants at 100 μ M. There was no change between the control LDH/ADH samples and the samples exposed to HOCl after being combined with GSH. These results suggest that at reasonable cellular levels of GSH, both HOCl and caffeic acid can be scavenged, and damage to LDH and ADH can be prevented. Despite this test, actual cellular contexts are much more complex and it is still reasonable to assume that in the case of bursts of high levels of oxidative stress in disease states, LDH could be overwhelmed regardless of GSH presence.

CONCLUSION

This research shows that LDH is inhibited by low concentrations of HOCl and catechol-based ortho-quinones. Evidence from this research and other research in Dr. Landino's lab strongly suggests that cysteine residues on LDH are modified in the process of oxidation. Thus, in a disease context like Alzheimer's, high levels of HOCl generated near plaques by MPO is likely enough to severely hinder LDH viability in nearby neurons, and could contribute to irreparable energy loss in those regions. Since plaques can be present in the brain 10-15 years before the onset of symptoms, it is possible that HOCl damage to energy production in neurons occurs early as well.

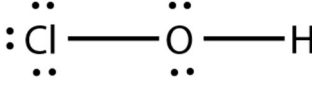
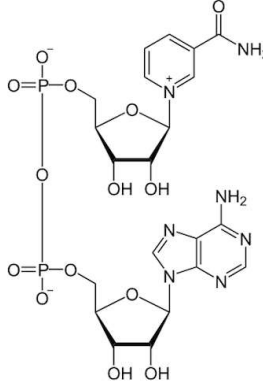
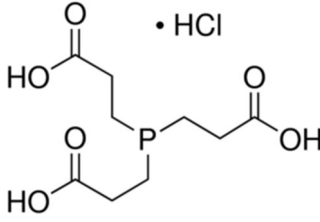
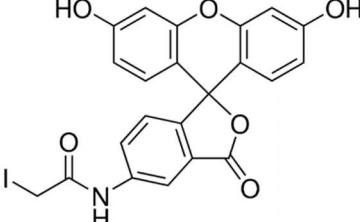
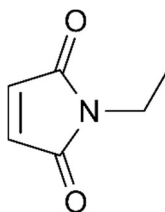
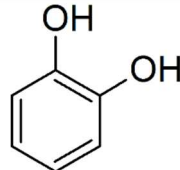
The results of this research also suggest that not all antioxidants are always effective at preventing oxidative damage, and can actually contribute to damage in states of high oxidative stress. Compounds like catechol and caffeic acid are abundant in foods and it is possible for them to be oxidized in the body after consumption. The resulting ortho-quinones can modify cysteine residues on important enzymes involved in energy production, like LDH. While these results are intriguing, there are still several more questions that need to be investigated. Namely, if these compounds do in fact modify cysteine residues on LDH and ADH *in vitro*, can we replicate this *in vivo*? Currently, Dr. Lisa Landino's lab at the College of William and Mary in Virginia is attempting to show that ADH is modified within yeast cells when exposed to these compounds. The lab is working on developing effective assays that can accurately determine if the compounds are bound to cysteine residues on a protein when using whole-cells or cell lysate.

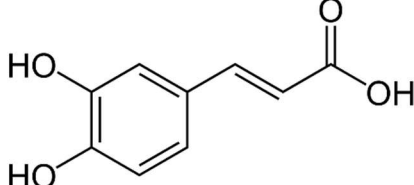
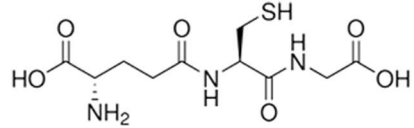
Additionally, it would be useful to do circular dichroism on LDH and ADH when they are exposed to these various oxidative compounds to determine more closely what specific conformation changes are occurring within the protein, and how each individual cysteine responds to its surrounding environment. More fluorescence data could also help determine how many cysteine residues are consistently modified by the various oxidizing agents. Lastly, it would also be useful to continue to expand the compounds used in the oxidizing process so that characterization of LDH and ADH responses can be more complete and extensive. See Appendix 3 for the full list of compounds and results regarding all oxidative agents used.

This research, and other research that is focused on glycolytic enzymes in the context of disease states is useful because it represents a type of basic research that has not been explored until recently and the results of which will contribute to understanding currently uncured diseases. In addition, studying the benefits and potential harms of antioxidants is relevant with respect to the current attention given to antioxidants as compounds that prevent the symptoms of ageing. Ageing and age-related diseases are not well understood. Research that addresses the basic underlying mechanisms of cell death in these contexts is needed to further understand how our body works in states of stress and redox instability.

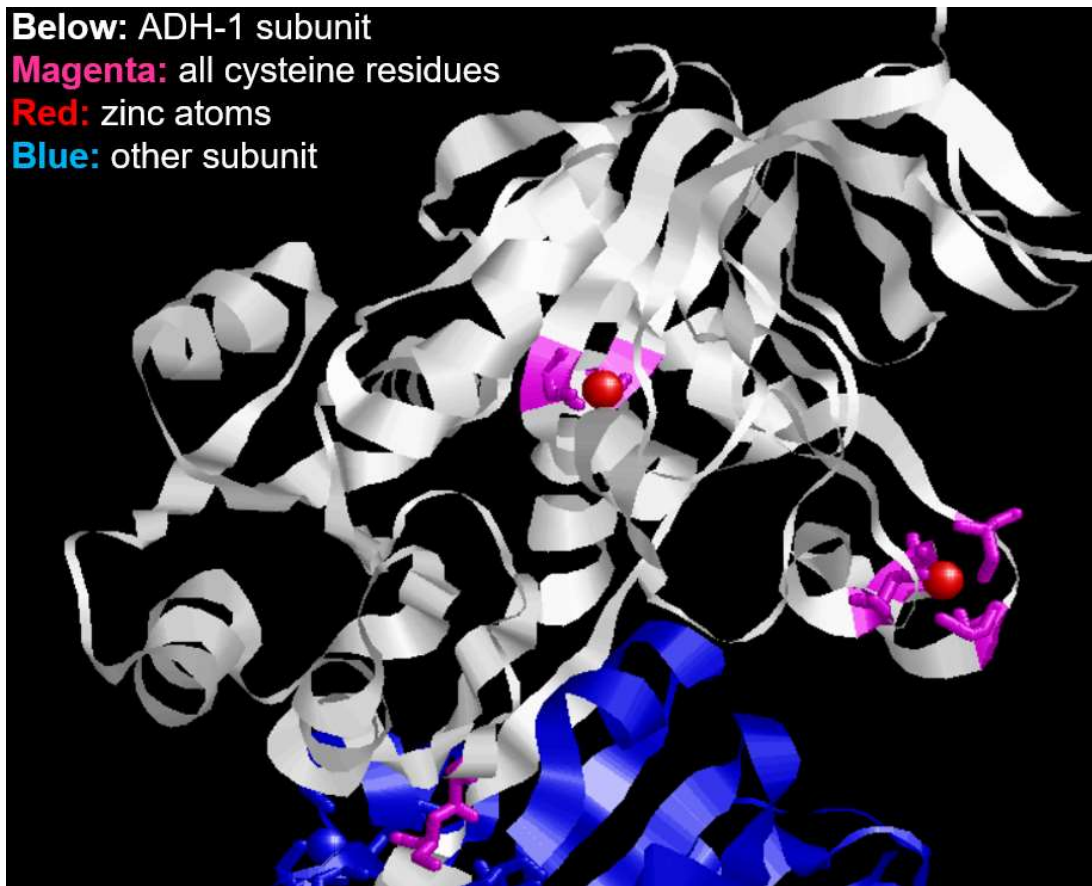
APPENDIX

Table of frequently used compounds, their structures, and abbreviations

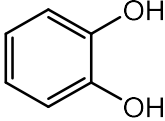
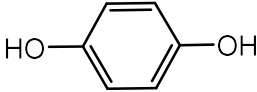
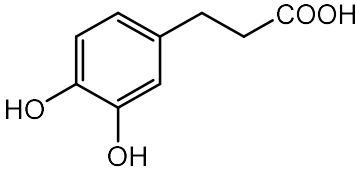
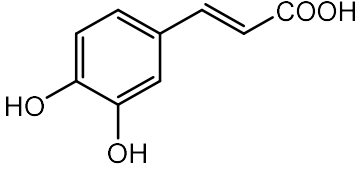
Compound	Structure	Abbreviation
Hypochlorous acid (bleach)		HOCl
Nicotinamide adenine dinucleotide		NADH (NAD ⁺)
tris(2-carboxyethyl)phosphine		TCEP
5-(Iodoacetamido)fluorescein		IAF
N-ethylmaleimide		NEM
Catechol		

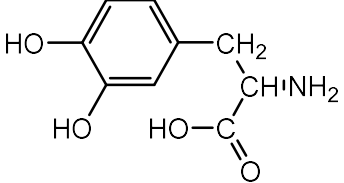
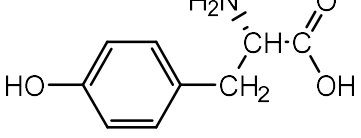
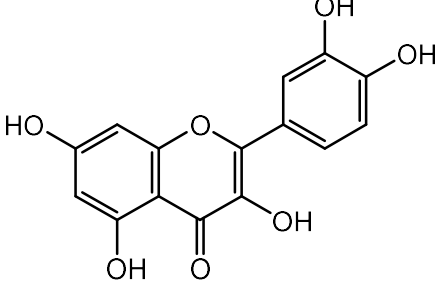
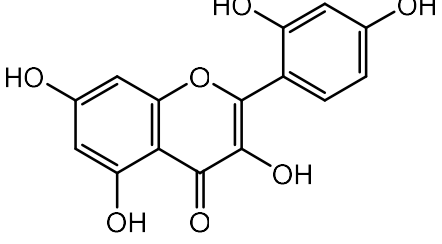
Caffeic Acid	 <p>The chemical structure of Caffeic Acid consists of a benzene ring with two hydroxyl groups (HO-) at the 3 and 4 positions. A propenoic acid side chain is attached to the 1 position of the ring, consisting of a double bond followed by a carboxylic acid group (-COOH).</p>	CA
Glutathione	 <p>The chemical structure of Glutathione is a tripeptide consisting of three amino acids: glutamic acid, cysteine, and glycine. The glutamic acid is at the N-terminus, followed by cysteine which has a free thiol group (-SH) on its side chain, and glycine at the C-terminus. The amino acid residues are linked by peptide bonds.</p>	GSH

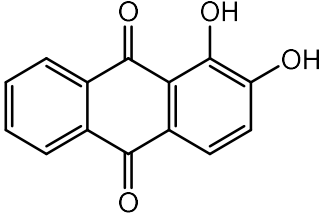
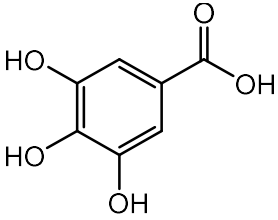
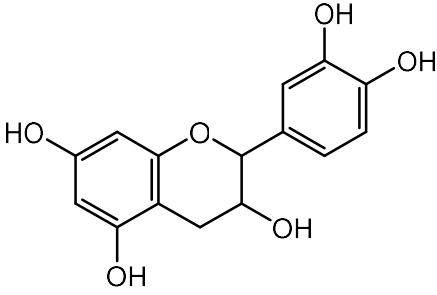
Yeast ADH structure with labeled important amino acids (PDB file 4W6Z)



All phenolic compounds oxidized and tested for inhibition properties with LDH and ADH

Compound Structure	Compound Name and Information	LDH (% inhibition with and without tyrosinase "E")	ADH (% inhibition with and without tyrosinase "E")
	catechol MW = 110.11 Solubility: 430 g/L H ₂ O	LDH assay Without E: 100uM → 0 +/- 5% With E: 100uM → 80 +/- 15%	ADH assay Without E: 100uM → 0 +/- 10% With E: 100uM → 100 +/- 2%
	1,4-dihydroxybenzene (hydroquinone) MW = 110.11 Solubility: 6.72 g/L H ₂ O	LDH assay: Without E: 100 uM → 10 +/- 10% With E: 100uM → 5 +/- 10%	ADH assay Without E: 100uM → 0 +/- 10% With E: 100uM → 100 +/- 2%
	hydrocaffeic acid MW = 182.18 Solubility: 428 mg/mL H ₂ O	LDH assay: Without E: 100uM → 30 +/- 10% With E: 100uM → 80 +/- 10%	ADH assay Without E: 100uM → 0 +/- 10% With E: 100uM → 100 +/- 2%
	caffeic acid MW = 180.18 CAS 331-39-5 7 mg/mL DMF	LDH assay: Without E: 100uM → 20 +/- 10% With E: 100uM → 75 +/- 10%	ADH assay Without E: 100uM → 0 +/- 0.1% With E: 100uM → 100 +/- 0.1%

	<p>L-dopa MW = 197.19 Solubility: 5 mg/mL H₂O</p>	<p>LDH assay: Without E: 100 uM → 5 +/- 10% With E: 100uM → 25 +/- 2%</p>	<p>ADH assay Without E: 100uM → 0 +/- 5% With E: 100uM → 70 +/- 5%</p>
	<p>L-tyrosine MW = 181.19 Solubility: .453 mg/mL H₂O</p>	<p>Unable to dissolve</p>	<p>ADH assay Without E: 100uM → 0 +/- 10% With E: 100uM → 80 +/- 0.5%</p>
	<p>quercetin MW = 302.236 we have dihydrate so MW = 338.28 Solubility: 30 mg/mL DMF</p>	<p>LDH assay: Without E: 100uM → 30 +/- 5% With E: 100uM → 35 +/- 5%</p>	<p>ADH assay Without E: 100uM → 0 +/- 5% With E: 100uM → 0 +/- 2%</p>
	<p>morin MW = 302.236 Solubility: 50 mg/mL DMF</p>	<p>LDH assay: Without E: 100uM → 10 +/- 5% With E: 100uM → 60 +/- 5%</p>	<p>ADH assay Without E: 100uM → 5 +/- 5% With E: 100uM → 20 +/- 2%</p>

	<p>alizarin MW = 240.21 Solubility: .4 mg/mL H₂O 20 mg/mL DMF</p>	<p>LDH assay: Without E: 100 uM → 5 +/- 2% With E: 100uM → 20 +/- 2%</p>	<p>ADH assay Without E: 100uM → 0 +/- 20% With E: 100uM → 0 +/- 2%</p>
	<p>gallic acid MW = 170.12 g/mol Solubility: 11.9 mg/mL H₂O 25 mg/mL DMF</p>	<p>LDH assay: Without E: 500uM → 5 +/- 10% With E: 500uM → 2 +/- 5%</p>	<p>ADH assay Without E: 100uM → 0 +/- 10% With E: 100uM → 5 +/- 5%</p>
	<p>catechin MW = 290.271 g/mol Solubility: 100 mg/mL DMF</p>	<p>LDH assay: Without E: 100uM → 0 +/- 15% With E: 100uM → 35 +/- 5%</p>	<p>ADH assay Without E: 100uM → 0 +/- no error With E: 100uM → 20</p>
	<p>EGCG MW: 458.4 g/mol Solubility: 25 mg/mL DMF Present in: green tea Biological effect: chemoprevention</p>	<p>LDH assay: Without E: 100uM → 20 +/- 5% With E: 100uM → 45 +/- 2%</p>	<p>ADH assay Without E: 100uM → 0 +/- 5% With E: 100uM → 10 +/- 2%</p>

T.J.'s Organic Green Tea



Extraction:
1.94g/100mL

LDH assay:
Without E:
Raw extract →
94 +/- 2%
With E:
Raw extract →
98 +/- 2%

ADH assay
Without E:
Raw Extract →
28 +/- 2%
With E:
Raw extract →
55 +/- 5%

Yogi Green Tea Kombucha

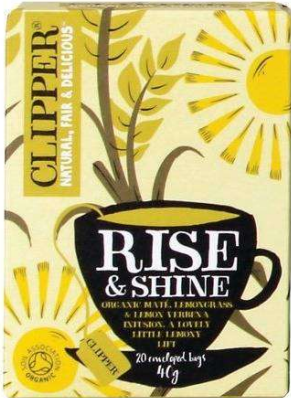


Extraction:
1.94g/100mL

LDH assay:
Without E:
Raw extract →
50 +/- 8%
With E:
Raw extract →
80 +/- 5%

ADH assay
Without E:
Raw Extract →
15 +/- 3%
With E:
Raw extract →
35 +/- 3%

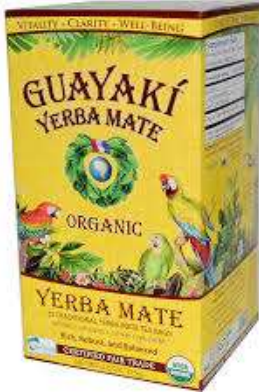

Clipper Rise and Shine (Herbal)



Extraction:
2.04g/100mL

LDH assay:
Without E:
Raw extract → 0
+/- 2%
With E:
Raw extract →
78 +/- 2%

ADH assay
Without E:
Raw extract →
0 +/- 7%
With E:
Raw extract →
100 +/- 0.5%

<p>Yerba Mate (Herbal)</p> 	<p>Extraction: 3.09g/100mL</p>	<p>LDH assay: Without E: Raw extract → 7 +/- 4% With E: Raw extract → 78 +/- 2%</p>	<p>ADH assay: Without E: Raw extract → 0 +/- 5% With E: Raw extract → 100 +/- 1%</p>
<p>PP60 Green Tea Extract</p>	<p>0.2 mg/mL (in rxn)</p>	<p>LDH assay: Without E: 0.2mg/mL → 87 +/- 4% With E: 0.2mg/mL → 93 +/- 2%</p>	<p>ADH assay: Without E: 0.2mg/mL → 30 +/- 25% With E: 0.2mg/mL → 55 +/- 10%</p>
<p>German Hallertau HOPs (2.5% alpha)</p> 	<p>Extraction: 1.0g/50mL</p>	<p>LDH assay: Without E: Raw extract → 22 +/- 7% With E: Raw extract → 84 +/- 2%</p>	<p>ADH assay: Without E: Raw extract → 0 +/- 2% With E: Raw extract → 55 +/- 5%</p>

<p>Cascade HOPs (8.4% alpha, 7.5% beta)</p> 	<p>Extraction: 1.0g/50mL</p>	<p>LDH assay: Without E: Raw extract → 13 +/- 6% With E: Raw extract → 72 +/- 2%</p>	<p>ADH assay: Without E: Raw extract → 0 +/- 15% With E: Raw extract → 40 +/- 2%</p>
<p>Apollo Hop Pellets (15-19% alpha, 5.5-8% beta)</p> 	<p>Extraction: 1.0g/50mL</p>	<p>LDH assay: Without E: Raw extract → 5 +/- 2% With E: Raw extract → 50 +/- 4%</p>	<p>ADH assay: Without E: Raw extract → 0 +/- 2% With E: Raw extract → 25 +/- 2%</p>

Rabbit muscle LDH single subunit amino acid sequence (PDB 3H3F)

AALKD QLIHN LLKEE HVPQN
KITVV GVGAV GMACA ISILM
KDLAD ELALV DVMED KLKGE
MMDLQ HGSLF LRTPK IVSGK
DYSVT ANSKL VIITA GARQQ
EGESR LNLVQ RNVNI FKFII
PNVVK YSPHC KLLVV SNPVD
ILTYV AWKIS GFPKN RVIGS
GCNLD SARFR YLMGE RLGVB
ALSCH GWILG EHGDS SVPVW
SGMNV AGVSL KTLHP ELGTD
ADKEQ WKQVH KQVVD SAYEV
IKLKG YTTWA IGLSV ADLAE
SIMKN LRRVH PISTM LKGLY
GIKED VFSLV PCVLG QNGIS
DVVKV TLTSE EEAHL KKSAD
TLWGI QKEL QF

Yeast ADH single subunit amino acid sequence (PDB 4W6Z)

IPETQ KGVIF YESHG KLEYK
DIPVP KPKAN ELLIN VKYSG
VCHTD LHAWH GDWPL PVKLP
LVGGH EGAGV VVGMM ENVKG
WKIGD YAGIK WLNGS CMACE
YCELG NESNC PHADL SGYTH
DGSFQ QYATA DAVQA AHIPQ
GTDLA QVAPI LCAGI TVYKA
LKSAN LMAGH WVAIS GAAGG
LGSLA VQYAK AMGYR VLGID
GGEGK EELFR SIGGE VFIDF
TKEKD IVGAV LKATD GGAHG
VINVS VSEAA IEAST RYVRA
NGTTV LVGMP AGAKC CSDVF
NQVVK SISIV GSYVG NRADT
REALD FFARG LVKSP IKVVG
LSTLP EIYEK MEKGQ IVGRY VVDTS
K

REFERENCES

- Bergmeyer HU. New values for the molar extinction coefficients of NADH and NADPH for the use in routine laboratories. *Z Klin Chem Klin Biochem*. November 1975. 13(11):507-508.
- Bolton JL, Dunlap T. Formation and Biological Targets of Quinones: Cytotoxic versus Cytoprotective Effects. *Chemical Research in Toxicology*, 2017. 30:13-37.
- Carocho M, Ferreira I. A review on antioxidants, prooxidants and related controversy: Natural and synthetic compounds, screening and analysis methodologies and future perspectives. *Food and Chemical Toxicology*. 2003. 51:15-25.
- Dalle-Donne I, Rossi R, Colombo R, Giustarini D, Milzani A. Biomarkers of Oxidative Damage in Human Disease. *Clinical Chemistry*. 2006. 52(4):601-623.
- Deng H, Zhadin N, Callender R. Dynamics of Protein Ligand Binding on Multiple Time Scales: NADH Binding to Lactate Dehydrogenase. *Biochemistry*. 2001. 40:3767-3773. Doi: 10.1021/bi0026268.
- Díaz I, de Castro IN, Medina MA. An experiment on the chemical modification of essential histidine residues of lactate dehydrogenase. *Biochemistry and Molecular Biology Education*. 1993. 21:219–223.
- Espinosa-Diez et. al. Antioxidant responses and cellular adjustments to oxidative stress. *Redox Biol*. 2015. 6:183-197. Doi: 10.1016/j.redox.2015.07.008.
- Foley TD, Cantarella KM, Gillespie PF, Stredny ES. Protein vicinal thiol oxidations in the healthy brain: not so radical links between physiological oxidative stress and neuronal cell activities. *Neurochemistry Research*. 2014. 39: 2030-2039.
- Giles NM, Giles GI, Claus J. Multiple roles of cysteine in biocatalysis. *Biochemical and Biophysical Research Communications*. 2003. 300:1-4.
- Green PS. et. al. Neuronal expression of myeloperoxidase is increased in Alzheimer's disease. *Journal of Neurochemistry*. 2004. 90(3):724-733. Doi: 10.1111/j.1471-4159.2004.02527.x.

- Halliwell B. Are polyphenols antioxidants or pro-oxidants? What do we learn from cell culture and in vivo studies? *Archives of Biochemistry and Biophysics*. 2008. 476:107-112.
- Hillion M, Antelmann H. Thiol-based redox switches in prokaryotes. *Biological Chemistry*. 2015. Doi: 10.1515/hsz-2015-0102.
- Iba M, Guo JL, McBride JD, Zhang B, Trojanowski JQ, Lee VM. Synthetic Tau Fibrils Mediate Transmission of Neurofibrillary Tangles in a Transgenic Mouse Model of Alzheimer's-like Tauopathy. *JNeurosci*. 2013. 33(3):1024-1037. Doi: 10.1523/JNEUROSCI
- Kim J, Dang C. Multifaceted roles of glycolytic enzymes. *Trends in Biochemical Sciences*. 2005. 30:142-150.
- "Latest Alzheimer's Facts and Figures." Latest Facts & Figures Report: Alzheimer's Association. 29 Mar. 2016. Web. 21 Feb. 2017. <<http://www.alz.org/facts/overview.asp>>
- Lobo V, Patil A, Phatak A, Chandra N. Free radicals, antioxidants, and functional foods: Impact on human health. *Pharmacognosy Reviews*. 2010. 4(8):118-126.
- Lu JM, Lin PH, Yao Q, Chen C. Chemical and molecular mechanisms of antioxidants: experimental approaches and model systems. *Molecular Medicine*. 2010. 14(4):840-860.
- Lushchak V. Glutathione Homeostasis and Functions: Potential Targets for Medical Interventions. *Journal of Amino Acids*. 2012. Doi: 10.1155/2012/736837.
- McClendon S, Zhadin N, Callender R. The approach to the Michaelis complex in lactate dehydrogenase: the substrate binding pathway. *Biophys J*. 2005. 89(3):2024-2032. Doi: 10.1529/biophysj.105.062604.
- National Institute on Aging, Scientific Images. March 15, 2017. Web. March 16, 2017. <<https://www.nia.nih.gov/alzheimers/scientific-images>>
- Pineda JR, Callender R, Schwartz S. Ligand Binding and Protein Dynamics in Lactate Dehydrogenase. *Biophys J*. 2007. 93(5): 1474-1483. Doi: 10.1529/biophysj.107.106146.
- Pocernich CB, Butterfield DA. Elevation of glutathione as a therapeutic strategy in

- Alzheimer's disease. *Biochem Biophys Acta*. 2012. 1822(5):625-630. Doi: 10.1016/j.bbadis.2011.10.003.
- Poole LB. The basics of thiols and cysteines in redox biology and chemistry. *Free Radical Biology and Medicine*. 2015. 80: 148-157.
- Powers JL, Kiesman NE, Tran CM, Brown JH, Bevilacqua VL. Lactate dehydrogenase kinetics and inhibition using a microplate reader. *Biochemistry and Molecular Biology Education*. July 2007. 35(4):287-292. Doi: 10.1002/bmb.74.
- Vander Heiden MG, Cantly LC, Thompson CB. Understanding the Warburg Effect: the Metabolic Requirements of Cell Proliferation. *Science*. 2009. 324(5930):1029-1033. Doi: 10.1126/science.1160809.
- Vlassenko A, Raichle M. Brain aerobic glycolysis functions and Alzheimer's disease. *Clinical and Translational Imaging*. 2014. 3:27-37.
- Whiteman M. et al. Hydrogensulfide: a novel inhibitor of hypochlorous acid-mediated oxidative damage in the brain?. *Biochemical and Biophysical Research Communications*. 2005. 326:794-798.
- Yap Y. et al. Hypochlorous acid induces apoptosis of cultured cortical neurons through activation of calpains and rupture of lysosomes. *Journal of Neurochemistry*. 2006. 98:1597-1609.

Thank you to the Charles Center at William & Mary, Pete and Sandra Bracken, and the English-Stonehouse Fellowship for aiding in the funding of this project.

Thank you to Dr. Lisa Landino for being an invaluable advisor and mentor.

And lastly, thanks to CW, a dear friend.